



RESEARCH ARTICLE

COVID-19: A Global and Mathematical Perspective

Richard R. Zito, Ph.D

Richard R. Zito Research LLC;
Tucson, Arizona, USA



OPEN ACCESS

PUBLISHED

28 February 2026

CITATION

Zito, R.R., 2026. COVID-19: A Global and Mathematical Perspective. Medical Research Archives, [online] 14(2).

COPYRIGHT

© 2026 European Society of Medicine. This is an open- access article distributed under the terms of the Creative Commons Attribution License, which permits unrestricted use, distribution, and reproduction in any medium, provided the original author and source are credited.

ISSN

2375-1924

ABSTRACT

This publication describes the global spread of COVID-19 in mathematical terms from its beginning in Wuhan, China. Using the techniques of graph theory and matrix algebra, the airports servicing Seoul and London are identified as most in need of passenger screening to prevent the global spread of infectious disease by air travelers during a pandemic. Furthermore, it is the *trace* of powers of the *adjacency matrix* – which is the matrix that characterizes the network of flights connecting cities on a regional or global scale – that is proportional to the *infection risk* of any given network of flights. It will be demonstrated that relatively small network changes can result in a significant reduction of infection risk, with a minimal reduction of passenger throughput. The infection risk posed by population migration is more difficult to characterize than that posed by air travel, although the two are related. However, *chaos theory* suggests that once the infectiousness of a disease (as measured by the *reproduction number*, the number of people that each sick person can infect in a fully susceptible population) exceeds a threshold of about 4, the future number of active cases becomes difficult to predict; a phenomenon that is exacerbated by extreme *sensitivity to initial conditions*. That is to say, individual cases can make large changes in the future course of a pandemic, making accurate long-term prediction impossible.

Keywords: COVID-19, air travel, migration, adjacency matrix, chaos theory.

Introduction

In many ways the COVID-19 pandemic is unique in the annals of medicine. COVID is one of the most infectious diseases known – measles, the most infectious disease known, is slightly worse. This, combined with rapid inexpensive intercontinental air travel and global mass migrations, produced unprecedented conditions ideal for the spread of disease. As COVID spread, science watched, and never before has there been so much data available to biochemists, molecular biologists, geneticists, physicians, and mathematicians, from the very beginning of its onset. This publication will concentrate on the mathematics of that spread. Graph theory and matrix algebra will be used to identify global “hot spots” requiring monitoring for the early detection of infectious diseases. Furthermore, the chaotic behavior of recursive equations and systems of nonlinear differential equations seems to explain some of the quasi-erratic features of the COVID pandemic due to the uncontrolled migration of people; especially into Europe from Africa and the middle east, as well as across the southern border of the U.S. Unfortunately, this same chaotic behavior may also preclude accurate long-term predictions for the course of any pandemic in the same way that accurate long-term weather forecasting is forbidden.

The Beginning of the COVID-19 Pandemic

The COVID-19 pandemic began at the Huanan Seafood Market in Wuhan, China. Examination of Figure 1 explains why this conclusion is so certain. Notice how half of the first 155 infections (December 2019) were clustered around the Huanan Market, with only 19 infections (12.26%) observed on the other side of the Yangtze River where the Wuhan Institute of Virology was located.¹ Although some have suspected the Institute as the source of the infection, the probabilities are greatly against this hypothesis since it wasn't until February 2020 that 3 cases appeared near the Institute.¹ By then Wuhan had experienced a total of hundreds of cases of COVID-19.¹

On December 26, 2019, Dr. Zhang Jixian of “The Second Hospital of Hebei Medical University Shijiazhuang, China”, a veteran of the 2003 SARS outbreak, observed in the CT thorax images of two elderly patients, differences from pneumonia caused by common viruses. Further examination of the couple's son also showed the same abnormalities in the CT scan, as did another patient admitted on December 27 from the Huanan Seafood Market.² Patient isolation measures began almost immediately. Although the identity of the true “patient zero”, the first person to have been infected in the COVID-19 pandemic in Wuhan, China, remains unconfirmed and the subject of debate, a study by Michael Worobey suggests it was a female seafood vendor at the Huanan Seafood Wholesale Market with symptom onset on December 11, 2019.³ In any case, the pandemic had certainly begun.

So, how did an infection that started at a seafood market in China spread over the entire planet and, as of April 13, 2024, infected 704,753,890 million people (confirmed cases), and killed just over 7 million globally?⁴ In a world of almost 8 billion people, that's about 9% of the Earth's population infected and 0.09% dead. The answer is basically *AIR TRAVEL* and *MIGRATION!*

The Trouble with Travel

When people travel they take their diseases with them, and the United States- an economic power situated between the economic powers of Europe and Asia - bears a particularly heavy responsibility when it comes to preventing the global spread of disease in general. Figure 2 is a simplified map of the direct (non-stop) air routes (links) of several major air lines connecting the capital cities of the Pacific Rim and the North Atlantic with U.S. coastal ports of entry.

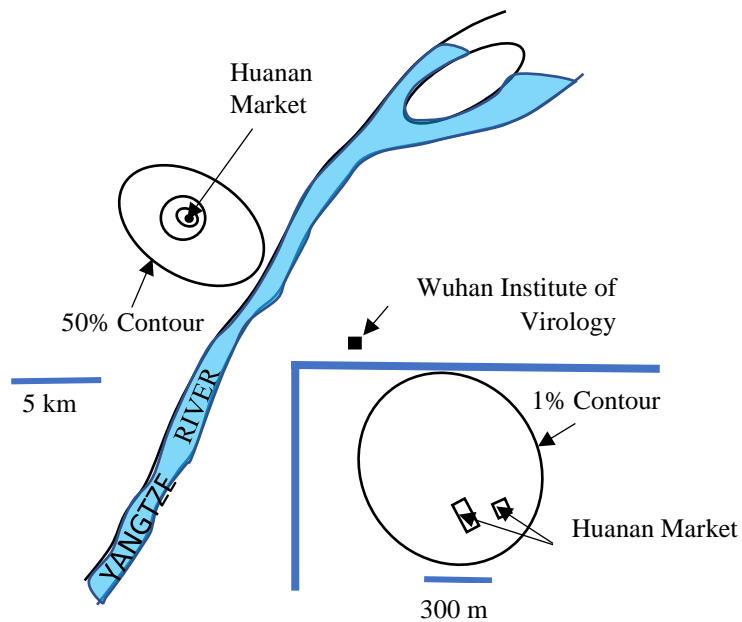


Figure 1 – Schematic map of Wuhan, China. A time “snap-shot” at the beginning of the COVID pandemic.¹ The 1% and 50% contours mean that 1% and 50% of all the confirmed cases occurred within those contours, respectively.

Tokyo Japan, Beijing China and Seoul South Korea were used to represent Asia. This is convenient because the major carriers Japan Air Lines (JAL),⁵ Air China (AC),⁶ and Korean Air (KA),^{7,8} respectively, have their hubs in these cities. Representing the U.S. is more difficult. It will be assumed that Seattle, San Francisco, and Los Angeles represent the most common points of entry into the U.S. from Asia because they are the closest major cities. Furthermore, the major carrier Delta Air Lines (Δ) will be used to represent the U.S. routes to Asia.⁹

Around the North Atlantic, Western Europe will be modeled by London UK, Paris France, and Munich Germany, which are hubs for British Airways (BA)¹⁰, Air France (AF)¹¹, and Lufthansa (L)¹². Again, representing the U.S. will be more difficult because of its size, but New York and Washington D.C. will be chosen as models for the East Coast. The proximity of these cities to Europe, and their importance, suggests that there will be a great deal of human traffic between these two American cities and the economic/industrial/tourism capitals of Europe. As before, Delta Airlines (Δ) will be used to represent air traffic from the U.S. to Europe.

The Carrier Flight Adjacency Matrix

The air routes in Figure 2 can be reduced to two simple *graphs*. One representing the Pacific Rim, and the other representing the North Atlantic (Figure 3). Ultimately, from each of these graphs, a mathematical object that will be called a *total flight adjacency matrix* will be constructed. However, it will be helpful if an intermediate matrix, that will be called a *carrier flight adjacency matrix*, is constructed first. The entries of the carrier flight adjacency matrix (Figures 4 and 5) are just the *number of direct non-stop round-trip daily flights from the hubs of the carriers cited above to another air-adjacent city*.

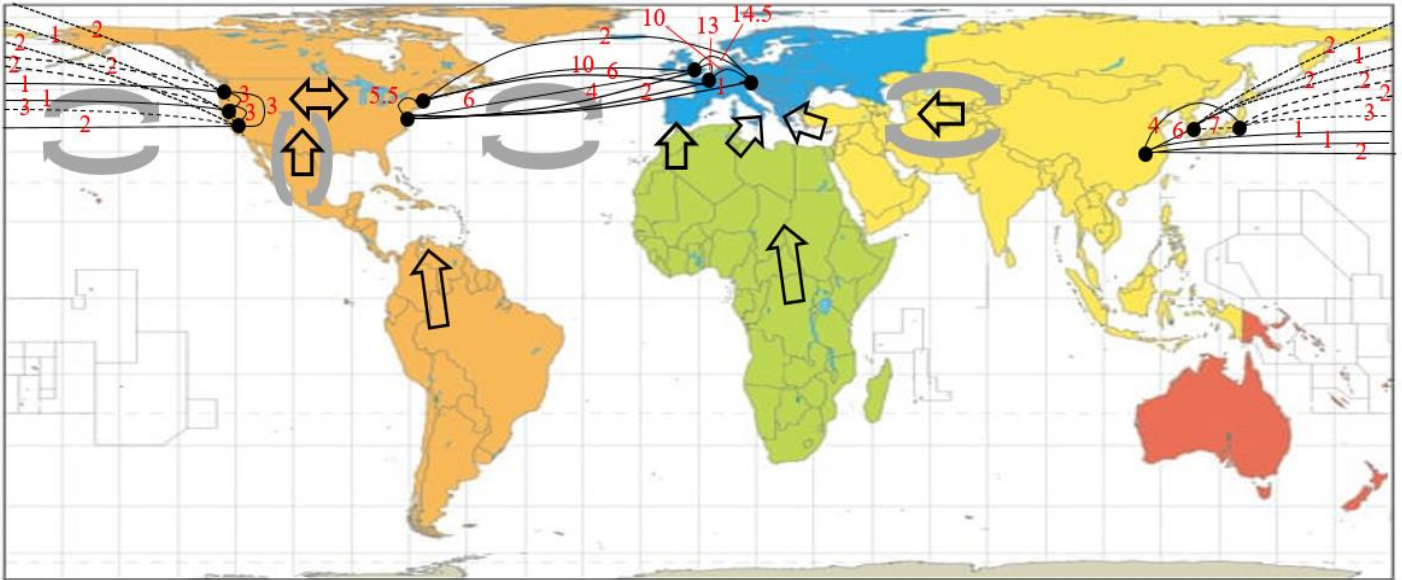


Figure 2 – Our connected world. Black dots represent major cities that are directly connected by air travel. The black arcs (solid, dashed, and dotted for clarity) represent the air routes between two cities, and the red numbers on them represent the *total* number of direct, non-stop, round-trip flights available to travelers from *all* of the transoceanic carriers considered. The arrows in black outline represent routes of population migration (both legal and illegal). The gray curved arrows indicate that there is a circulation of infected people traveling back and forth between nations. Air travel from the U.S. provides a convenient short-cut for disease, connecting Europe’s west coast with Asia’s east coast. The network of interactions depicted will be dissected into components.



Figure 3 – A) Graph of flights for the Pacific Rim. B) Graph of flights for the North Atlantic. As in Figure 2, the red numbers represent the *total* number of *direct, non-stop, round-trip daily flights* from *all* carriers connecting any two given cities. Only direct flights need to be considered because indirect routes, say Beijing to Tokyo to Seattle, can be constructed from the direct flights.

TO:

| | Tokyo | Beijing | Seoul | Seattle | San Francisco | Los Angeles |
|-----------------------------|-------|---------|-------|---------|---------------|-------------|
| Tokyo (JAL/KA) | 0 | 2 | 3 | 1 | 2 | 2 |
| Beijing (AC) | 2 | 0 | 3 | 1 | 1 | 1 |
| Seoul (KA/Δ) | 4 | 3 | 0 | 2 | 1 | 2 |
| Seattle (Δ/KA) | 1 | 0 | 2 | 0 | 3 | 3 |
| San Francisco (Δ/KA) | 0 | 0 | 1 | 3 | 0 | 3 |
| Los Angeles (Δ/KA) | 1 | 1 | 2 | 3 | 3 | 0 |

FROM: A_P^C

Figure 4 – The Pacific Rim Carrier Adjacency Matrix (A_P^C). The numerical entries (matrix elements) are the typical number of *direct, non-stop, round-trip daily flights* of various carriers (bold type) from their home-base “hub” city to another city, and are denoted by their “from-to” cities, or row and column numbers. For example, the element $A_P^C(\text{Tokyo, Seattle}) = A_P^C(1,4) = 1$. Notice that the shaded blue rectangle covers only zeros along the “main diagonal”

of the carrier adjacency matrix. That's because there are no air routes from any given city to itself. Notice also that this adjacency matrix is *not* symmetric across the main diagonal. That's because a carrier from one hub that flies to another destination city may not have the same number of direct, non-stop, round-trip flights as a carrier based in the destination city has to the first hub. Further complications arise because some air lines are "partners", while others are not. So, although both JAL and Δ both have a partner relationship with KA, there is *no direct* partnering between JAL and Δ . Therefore, JAL has two flight from Tokyo to Los Angeles, while Δ has only one (independent) flight from Los Angeles to Tokyo; for a total of three flights (see Fig's 2 and 3). Strangely, KA runs an extra flight between Seoul and Tokyo independent of JAL. By contrast, Δ and KA are partners. Therefore, the two KA flights between Seoul and Los Angeles are the same as the two Δ flights between Los Angeles and Seoul for a total of just two physical flights (not four) – see Fig's 2 and 3. The complex partnering relationships are summarized to the right of the departure cities (normal type after '/'). The colored boxes group independent flights from Asia to an American city of the same color heading. Note that direct, non-stop, round-trip flights between two non-hub cities of a given carrier, will not be considered because it is awkward to supply aircraft to such a route. For example, there are no direct, non-stop, AC round-trip flights between Tokyo and Seoul, etc.

The carrier flight adjacency matrix of Figure 4 suggests that on the West Coast of the U.S., Los Angeles is the most dangerous city with regard to the introduction of infections from Asia. The reason is because it is connected by the largest number of flights to Asia (the sum of the numbers in the red boxes is $2 + 1 + 2 + 1 + 1 = 7$ flights per day). Next comes Seattle, with a total number of flights (blue boxes) equal to $1 + 1 + 2 + 1 = 5$ flights per day. Finally, San Francisco is safest with only $2 + 1 + 1 = 4$ flights per day (black box). What actually happened was that Seattle was infected first, followed almost simultaneously by Los Angeles. A situation not unexpected given the size of the elements of A_P^C .

There is very little public information available about U.S. "patient zero" because he understandably wishes to remain anonymous. Although patient zero was the first person in the U.S. positively recognized to have COVID-19, it might have been circulating unrecognized on the West Coast of the U.S. for a few weeks before that. What has been published is that patient zero was a 35-year old male, he checked himself into a clinic on January 19, just four days after arriving in Seattle on an "indirect flight" from Wuhan China.^{13,14} Seattle's patient zero (synonymous with patient zero for the U.S.) was initially quarantined in an Ebola-type enclosure, but was eventually released when he was deemed to be non-infectious on February 21, 2020 (33 days after arrival at the

clinic – *very safe*). However, COVID continued to spread in the Seattle area. This suggests that one or more of patient zero's contacts was missed, or that a second vector was introduced into the area!

In Los Angeles county, patient zero was Qian Lang, a 38-year-old salesman whose wife's mother lived in Wuhan, China.¹⁵ He was also U.S. patient 4, and was eventually hospitalized at Cedars-Sinai Medical Center after experiencing a severe fever on January 22, 2020.¹⁵ It should be noted that the travel-ban from China to the U.S. did not take effect until 5 PM EST on February 2, 2020. Furthermore, it would not have applied to either patient zero anyway since citizens and lawful permanent residents of the U.S. and their immediate relatives were exempt. In short, the travel ban was *too late and too porous* to prevent disease from entering the U.S.¹⁶

Wuhan is not well connected by air, and arriving at a hub in time for a departing international flight to Seattle is problematic. However, one possible path that avoids excessive layovers but provides adequate aircraft transfer time might be something like flying China Eastern Airlines from Wuhan to Tokyo, followed by a JAL flight to Seattle departing at about 6:10 PM on January 15, 2020 and arriving in Seattle at about 9:55 AM, also on the 15th after crossing the International dateline. Perhaps patient zero had something to eat during his layover in Tokyo; assuming

he really did travel that way? Perhaps he unknowingly infected others in that airport? Although, this seems unlikely since the flight from Tokyo to Seattle is about 9 hours, putting him in Tokyo about four and a half days before the onset of clinical symptoms. Typically, a person displays clinical symptoms 5 days *after* infection.¹⁷ Therefore, patient zero was probably infected just before he left Wuhan, and would have had a very low virion titer. Without coughing or sneezing, transmission seems unlikely, although technically he would have been an incubation carrier. However, the infection of others after arriving in Seattle prior to hospitalization *is* likely – much more likely than remaining infectious after quarantine, when his antibody titer was near maximum and he was no longer symptomatic. The travel scenario presented here is speculative, but it does match what matrix elements $A_P^C(1,4) + A_P^C(4,1) = 2$ suggest to be a high probability route for how COVID reached the West Coast of the U.S. Only travel to Los Angeles from Tokyo is riskier; $A_P^C(1,6) + A_P^C(6,1) = 3$. Something similar to this reconstruction of events may have actually taken place. *The establishment of the Traveler-based Genomic Surveillance program in Seattle-Tacoma International Airport, LAX, and San Francisco International Airport, by the U.S. government*

*will facilitate early detection of infectious diseases introduced into the West Coast of the U.S. from Asia.*¹⁸ This recent very important step was taken far *too late* to have prevented the spread of the COVID-19 pandemic in the U.S., but it will be a vital link in the chain of infectious disease defenses going forward into the future. What about the circulation of disease in the other direction? How did the COVID infection reach the East Coast of the U.S.?

The situation on the east coast of the U.S. is more confusing. Sometime in February 2020 (between 12 and 40 days after Seattle’s patient zero was hospitalized), Lawrence Garbuz became the New York metropolitan area’s COVID “patient zero”^{19, 20} - but what strain? The claim is that the alpha strain (PANGO B.1.1.7) did not appear in Kent, England until September of 2020 (1,108 cases by Sept. 13)!²¹ Furthermore, Garbuz is known not to have been traveling. Therefore, frighteningly, he must have been infected indirectly by an unknown carrier who had an even *earlier* infection. In any case, by late November 2020 alpha strain had spread to the U.S., and by January 2021 thirty states were involved in the infection.²² Figure 5 below is the North Atlantic carrier adjacency matrix corresponding to Figure 3B.

| | | TO: | | | | |
|-----------------|-----------------|--------|-------|--------|----------|---------------|
| | | London | Paris | Munich | New York | Washington DC |
| $A_A^C =$ FROM: | London (BA) | 0 | 7 | 6 | 8 | 6 |
| | Paris (AF/Δ) | 6 | 0 | 4.5 | 6 | 2 |
| | Munich (L) | 8.5 | 5.5 | 0 | 1 | 1 |
| | N.Y. (Δ/AF) | 2 | 3 | 1 | 0 | 5.5 |
| | Wash. DC (Δ/AF) | 0 | 0 | 0 | 5.5 | 0 |

Figure 5 – The North Atlantic carrier flight adjacency matrix (A_A^C). Entries (elements) are the typical number of direct, non-stop, round-trip flights per day for the carriers chosen to represent North Atlantic air traffic. Note that Δ and AF are partners. Therefore, the total number of flights between New York and Paris is only 6 (3 of which are Δ flights); double counting of flights is not allowed. By comparison, the total number of flights between New York and London is 10 because Δ and BA are independent airlines. Note that some matrix elements are not integers. That is because some airlines do not fly between some cities every day, or they report a variable number of flights. In that case, a daily average must be used.

The sum of matrix elements $A_A(1,4)$ and $A_A(4,1)$ (for the BA and Δ carriers) is 10, the largest number of flights between New York and any other European city. This suggests that the UK would be the most probable source of COVID on the East Coast of the U.S. This appears to have been the case, at least as far as alpha was concerned.^{21, 22}

The Spread of COVID Across Eurasia

So, how did an infection that started out in Wuhan, China, manage to migrate across Eurasia to Kent, UK? The answer to this question comes from tracking numerous “patient zero” cases (Table 1). The trend is clear. COVID spread across Eurasia primarily through land and air travel into, and out of, China. Although some experts think that identifying “patient zero” individuals, for any particular region, is counter-

productive,²³ *they are wrong!*²⁴ The chain of patient zero individuals is one of the clearest pieces of evidence available for the spread of disease. No one is blaming anyone else, and although the first clinically documented cases may not be the very first actual cases, they are certainly some of the earliest; thereby giving a pretty clear indication of the spread direction. Waiting until an infection spreads further can create a misleading impression of the time sequence of events. Just because one population has a lower number of cases per capita than another neighboring population does not necessarily mean that they are in an earlier stage of pandemic, and therefore the second to be infected. Differences in isolation (both personal and national), as well as climate, and the natural resistance of a population, all affect case counts in a complex way.

Table 1 – The patient zero list for Eurasia.

‘Patient zero’ is defined as a local *resident* who has been *documented* as infected. Notice that the Middle East was infected more or less simultaneously, as was most of Europe (including Turkey). However, isolated cases, probably traceable to air travel as in the case of France, show that the whole world is in danger almost immediately after an outbreak anywhere.

| Country | Patient Zero Biography | Date of Onset of Symptoms | Reference Number |
|------------------------------|---|-------------------------------------|------------------|
| China | Female worker in Huanan market | Dec. 11, 2019 | 3 |
| Nepal | 32-year old male and student in Wuhan | Jan. 3, 2020 | 25 |
| India | 3 rd year medical student from Wuhan | Jan. 30, 2020 | 26 |
| Pakistan | 23-year old male | Feb. 26, 2020 | 27 |
| Iran | Unnamed merchant from Oom who traveled to China by air. | ~Feb. 19, 2020 | 28, 29 |
| Turkey | Male traveler to Europe! | Mar. 10, 2020 | 30 |
| Continental Europe: Spain | A pregnant female in Spain. | Mar. 4, 2020 | 31 |
| France | 42-year old male. Possibly the first case in continental Europe. Wife worked near airport. | Dec. 27, 2019 | 32 |
| Italy | 38-year old male from Codogno, Lombardy. | Feb. 21, 2020 | 33 |
| UK | No patient zero identified. Infections introduced on at least 1100 occasions, mostly from Spain, France, and Italy. | ¿Early Sept. 2020 for alpha strain? | 21, 34 |

The globe has now been spanned, and the spread of COVID within the U.S. has been discussed in detail in the literature.³⁵ Although a carrier adjacency matrix may seem to be just a very convenient way of organizing data, it can be used to generate a more general type of adjacency matrix for *all* flights between any two cities, regardless of carrier. This *total flight adjacency matrix* has many desirable mathematical properties that allow the epidemiologist to answer certain types of questions relevant to the spread of disease. In fact, the total flight adjacency matrix is so useful that it would be a great help for detecting and managing the global spread of infectious diseases if it were expanded to include all the Earth's cities, airline routes, flights, and the exact number of passengers on each flight. Extracting all the information available from such a large matrix is a job for a super-computer.

The Total Flight Adjacency Matrix

From the discussion above, and the caption to Figure 4, the elements of the *total flight adjacency matrix*

(denoted by A_P and A_A for the Pacific Rim and North Atlantic respectively – *note that the superscript 'C' has been removed*) is constructed as follows. Let i and j be integers used to identify the row and column of any two hub cities, *then the (i,j) element of the total flight adjacency matrix is just the sum of the (i,j) and (j,i) elements of the carrier flight adjacency matrix when the carriers based in the i and j hubs are independent. If the carriers based in the i and j hubs are "partners", then the (i,j) element of the total flight adjacency matrix is equal to the larger of the (i,j) and (j,i) , elements of the carrier flight adjacency matrix; these latter two elements are usually, but not always, equal to each other* (e.g. see Figure 4 caption). Therefore, the (i,j) and (j,i) elements of the total flight adjacency matrix are also equal to each other (i.e. the total flight adjacency matrix is symmetric with respect to round-trips, or "one-way" legs as well). These simple rules prevent double counting of flights in the advent of alliances between airlines. Figure 6 shows the populated total flight adjacency matrices for the Pacific Rim and North Atlantic.

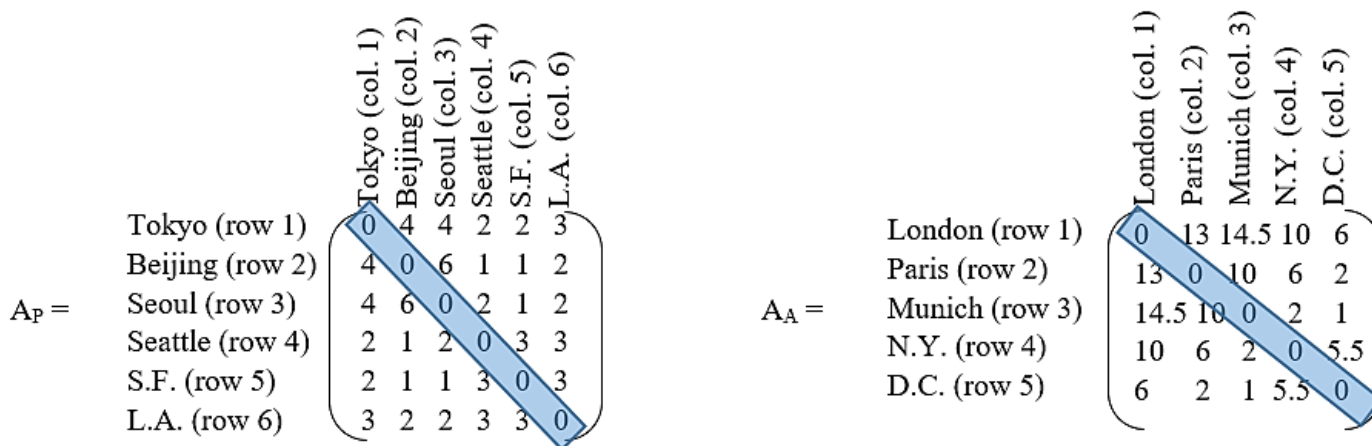


Figure 6 – Total flight adjacency matrices for the Pacific Rim and the North Atlantic. Compare the numbers in these matrices to those on the graphs of Figure 3.

If all the flight bookkeeping has been done correctly, the *total flight adjacency matrices* will be square and symmetrical with respect to the main diagonal of zeros; a useful arithmetic check. Note that exactly the same matrices apply to one-way legs of each round trip as well. Notice also that elements $A_P(1,6) + A_P(2,6) + A_P(3,6) = 7$, as they should (cf. Figure 4). That is to say, the number of direct, non-stop, round-trip flights from the three major Asian capitals into

Los Angeles is 7 per day; as previously determined. Also, the most dangerous route into the U.S. from Asia is Tokyo to L.A.; element $A_P(1,6) = 3$, as previously discussed. We are now ready to do some interesting calculations. Note that matrix elements may be any real number, but the results of calculations may be easier to understand if entries are rounded off to the nearest integer.

It should also be noted that there is a caveat associated with assuming that the spread of infection by air travel is proportional to the number of flights between cities. Namely, not all flights carry the same number of passengers. Some aircraft are larger than others, but carriers generally use the larger aircraft for flights between major cities, which are usually booked to capacity, or nearly so. The smaller planes are usually reserved for flights to smaller neighboring destinations. This limitation to the calculations that follow should be kept in mind. For now, it will be assumed that all flights are identical and carry the same *average* number of passengers.

The 'Paths', 'Cycles', 'Circuits' and 'Ways' of Travel

When people travel between two cities, they may not take the same flights over and over again. Scheduling difficulties, or traveling at different times, may require taking different flights. Furthermore, tourists may deliberately wish to stop at as many cities as possible before reaching a given destination and returning home. A natural question to ask is, "How many *paths* (direct or indirect) connect any two cities?". In Figure 3, cities were marked by "dots" called *vertices*, while airline routes were denoted by lines called *edges*. Edges have numbers on them or next to them, indicating that that one edge should also be replaced by multiple edges, each representing a round-trip flight (i.e. two flights, one going and one coming). However, the numbering scheme has been used to simplify the graphs. Otherwise 10 edges would have to be drawn just to connect N.Y. to London in Figure 3B. What a mess! Now, the word *path* has to be defined more carefully. Mathematically, *a path is just a sequence of edges* (also called a *walk* in the literature). In general, a path may use an edge (flight connection) more than once, and a vertex (city) may be visited more than once also. A path in which an edge (flight connection) is used only once will be called a *simple path* (also called a *simple chain* or a *simple edge sequence in the literature*).³⁶ In that case, once you board your departing flight, you are committed to finish your trip, and you can't go back

to get the medicine you may have forgotten! However, you may return to a hub city to depart to another city not yet visited (i.e. your journey may involve a "loop" – a colloquial term). Recasting the last question more precisely in terms of these *graph theory* definitions yields, "How many paths N-edges (N-flights) long connect any two given vertices (cities)?" This is the question that must be answered because the more paths that connect any two cities, the greater will be the potential for the spread of disease. As an example, consider Figure 3A. How many paths connect Beijing to Seattle that are two legs (2 edges, N = 2) long? The answer may surprise the reader. There is a theorem in graph theory that says the number of such paths between any two vertices (cities) of a graph is given by the matrix elements (entries) of the matrix $A^N = A^2$ (i.e. $A \bullet A$, where the "•" represents *matrix multiplications* as defined in mathematical handbooks, and where the symbol "A" *without any subscripts* has been used to represent either A_p or A_A).³⁶ When two matrices are matrix multiplied together, the elements of row *i* of the first matrix are multiplied by the elements of column *j* of the second.³⁷ The results of this arithmetic are then summed, and that sum is the value of the (i,j) element of the product. After a little work, all the elements of the product can be filled in. The result when $A = A_p$ is displayed in Figure 7.

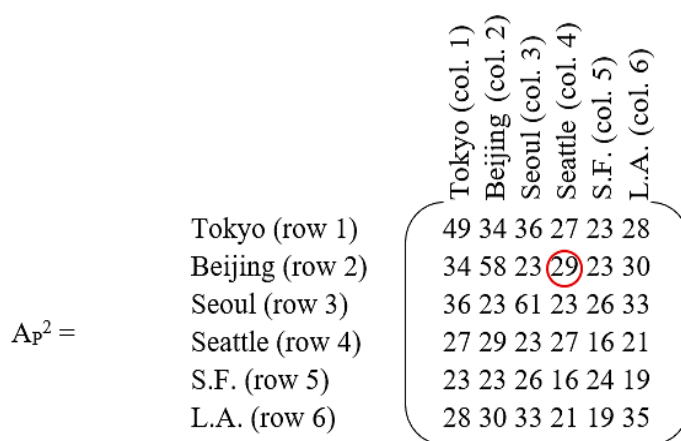


Figure 7 - The number of paths two edges long (1 stop or layover) for the Pacific Rim. The matrix element circled in red represents the number of paths available when travelling from Beijing to Seattle, WA.

The element circled in red indicates that there are 29 paths from Beijing to Seattle if a traveler is willing to make one stop to change planes. This result may seem baffling, but counting the paths will convince the reader of its veracity. There are 4 paths (flights) from Beijing to Tokyo, and two paths from Tokyo to Seattle – that makes $4 \times 2 = 8$ unique paths. There are 6 paths from Beijing to Seoul and two more paths from Seoul to Seattle – that makes another $6 \times 2 = 12$ paths. There is only one path from Beijing to San Francisco, but there are three paths from San Francisco to Seattle – so there are another three paths furnished by this sequence of flights. Finally, a traveler can go along two paths from Beijing to Los Angeles followed by another three paths to Seattle – that yields another $2 \times 3 = 6$ paths. Therefore, all total, there are $8 + 12 + 3 + 6 = 29$ distinct paths to get from Beijing to Seattle via one layover! Compare this to only one direct, non-stop, flight from Beijing to Seattle. The one-stop paths are more than an order of magnitude more common; and cheaper as well. U.S. patient zero used an indirect path. One should note that the main diagonal of the symmetrical matrix A_P^2 enumerates all possible round-trip *cycles* involving two legs; where a cycle is technically defined as any path that begins and ends at the same vertex (city). For example, Seoul has 61 such cycles that are two legs long, a maximum number for any of the cities considered. The reader may wonder how that can be, since Figure 3A shows only 6 direct, non-stop, round-trip daily flights connecting Seoul to Beijing,

4 to Tokyo, 2 to Seattle, 1 to San Francisco, and 2 to Los Angeles? It must be remembered that each round-trip has an outbound and a return leg. If the 6 round-trips to Beijing are labeled A, B, C, D, E, and F, then the outbound leg from any one letter can be matched with the return of any other. Possible outbound/return pairs could be AA, BB, CC, DD, EE, FF, AB, AC, AD, AE, AF, BA, CA, DA, EA, FA, BC, BD, BE, BF, CB, DB, EB, FB, CD, CE, CF, DC, EC, FC, DE, DF, ED, FD, EF, FE, for a sub-total of 36 cycles. However, there are also 16 cycles when commuting to Tokyo, 4 more cycles when going to and from Seattle, just 1 for San Francisco, and another 4 for Los Angeles, for a total of $36 + 16 + 4 + 1 + 4 = 61$ cycles. All these opportunities to spread disease make Seoul a likely city to be infected by travelers. A good place to *establish a WHO genomic surveillance center would be Incheon International Airport*, because it is so well connected by air to the airports of other major Pacific Rim cities. Similarly, calculation of A_A^2 implies that *London's Heathrow airport is a desirable outpost for a WHO genomic surveillance center in Europe*.

What about trips involving three legs (edges), or two layovers? Now how many paths exist between Beijing and Seattle? The general solution to this problem is given by A^3 , and requires one more matrix multiplication because $A^3 = A^2 \bullet A$. When $A = A_P$, $A_P^3 = A_P^2 \bullet A_P$. The result is displayed in Figure 8.

| | | | | | | | | | | | | | | | | | | | | | | | | | | | | | | | | | | | | | | | | | | | | | | | | | | |
|-----------------|---|----------------|------------------|---------------|-----------------|--------------|--------------|--|----------------|------------------|----------------|------------------|---------------|---------------|-----|-----|-----|-----|-----|-----|-----|-----|-----|-----|-----|-----|-----|-----|-----|-----|-----|-----|-----|-----|-----|-----|-----|-----|-----|-----|-----|-----|-----|-----|-----|-----|-----|-----|-----|-----|
| $A_P^3 =$ | <table border="0"> <tr><td>Tokyo (row 1)</td></tr> <tr><td>Beijing (row 2)</td></tr> <tr><td>Seoul (row 3)</td></tr> <tr><td>Seattle (row 4)</td></tr> <tr><td>S.F. (row 5)</td></tr> <tr><td>L.A. (row 6)</td></tr> </table> | Tokyo (row 1) | Beijing (row 2) | Seoul (row 3) | Seattle (row 4) | S.F. (row 5) | L.A. (row 6) | <table border="0"> <tr> <td style="writing-mode: vertical-rl; transform: rotate(180deg);">Tokyo (col. 1)</td> <td style="writing-mode: vertical-rl; transform: rotate(180deg);">Beijing (col. 2)</td> <td style="writing-mode: vertical-rl; transform: rotate(180deg);">Seoul (col. 3)</td> <td style="writing-mode: vertical-rl; transform: rotate(180deg);">Seattle (col. 4)</td> <td style="writing-mode: vertical-rl; transform: rotate(180deg);">S.F. (col. 5)</td> <td style="writing-mode: vertical-rl; transform: rotate(180deg);">L.A. (col. 6)</td> </tr> <tr> <td>464</td><td>518</td><td>533</td><td>357</td><td>333</td><td>437</td> </tr> <tr> <td>518</td><td>386</td><td>625</td><td>331</td><td>326</td><td>420</td> </tr> <tr> <td>533</td><td>625</td><td>420</td><td>394</td><td>324</td><td>423</td> </tr> <tr> <td>357</td><td>331</td><td>394</td><td>240</td><td>250</td><td>314</td> </tr> <tr> <td>333</td><td>326</td><td>324</td><td>250</td><td>200</td><td>287</td> </tr> <tr> <td>437</td><td>420</td><td>423</td><td>314</td><td>287</td><td>330</td> </tr> </table> | Tokyo (col. 1) | Beijing (col. 2) | Seoul (col. 3) | Seattle (col. 4) | S.F. (col. 5) | L.A. (col. 6) | 464 | 518 | 533 | 357 | 333 | 437 | 518 | 386 | 625 | 331 | 326 | 420 | 533 | 625 | 420 | 394 | 324 | 423 | 357 | 331 | 394 | 240 | 250 | 314 | 333 | 326 | 324 | 250 | 200 | 287 | 437 | 420 | 423 | 314 | 287 | 330 |
| Tokyo (row 1) | | | | | | | | | | | | | | | | | | | | | | | | | | | | | | | | | | | | | | | | | | | | | | | | | | |
| Beijing (row 2) | | | | | | | | | | | | | | | | | | | | | | | | | | | | | | | | | | | | | | | | | | | | | | | | | | |
| Seoul (row 3) | | | | | | | | | | | | | | | | | | | | | | | | | | | | | | | | | | | | | | | | | | | | | | | | | | |
| Seattle (row 4) | | | | | | | | | | | | | | | | | | | | | | | | | | | | | | | | | | | | | | | | | | | | | | | | | | |
| S.F. (row 5) | | | | | | | | | | | | | | | | | | | | | | | | | | | | | | | | | | | | | | | | | | | | | | | | | | |
| L.A. (row 6) | | | | | | | | | | | | | | | | | | | | | | | | | | | | | | | | | | | | | | | | | | | | | | | | | | |
| Tokyo (col. 1) | Beijing (col. 2) | Seoul (col. 3) | Seattle (col. 4) | S.F. (col. 5) | L.A. (col. 6) | | | | | | | | | | | | | | | | | | | | | | | | | | | | | | | | | | | | | | | | | | | | | |
| 464 | 518 | 533 | 357 | 333 | 437 | | | | | | | | | | | | | | | | | | | | | | | | | | | | | | | | | | | | | | | | | | | | | |
| 518 | 386 | 625 | 331 | 326 | 420 | | | | | | | | | | | | | | | | | | | | | | | | | | | | | | | | | | | | | | | | | | | | | |
| 533 | 625 | 420 | 394 | 324 | 423 | | | | | | | | | | | | | | | | | | | | | | | | | | | | | | | | | | | | | | | | | | | | | |
| 357 | 331 | 394 | 240 | 250 | 314 | | | | | | | | | | | | | | | | | | | | | | | | | | | | | | | | | | | | | | | | | | | | | |
| 333 | 326 | 324 | 250 | 200 | 287 | | | | | | | | | | | | | | | | | | | | | | | | | | | | | | | | | | | | | | | | | | | | | |
| 437 | 420 | 423 | 314 | 287 | 330 | | | | | | | | | | | | | | | | | | | | | | | | | | | | | | | | | | | | | | | | | | | | | |

Figure 8 - The number of paths three edges long (2 stops, or layovers) when travelling between any two major cities listed in the margins of the matrix A_P^3 .

The first take-away from this matrix is that the number of paths between major cities has now grown again by another order of magnitude with the addition of a second layover. Therefore, as the number of layovers grows arithmetically, the number of possible paths grows exponentially! *It may seem counter-intuitive but, unless all flights into a given country are forbidden (usually not practical) or travel restrictions are based on presence in an infected area within a specified time interval, cancellation of direct, non-stop, flights from an infected country may be the worst thing that can be done during a pandemic because it forces passengers, some of whom may be incubation carriers, into an enormous network of indirect flights to avoid flight restrictions; thereby maximizing the spread of disease. A better procedure is to channel as many travelers as possible into direct, non-stop, flights and test them before and after travel, with an appropriate quarantine period at each end.*

The route with the greatest number of travel options (and infection possibilities) is now Seoul to Beijing. *Again, Incheon International Airport would be a likely location for early detection of a new infectious strain.* However, some of the 625 possible travel itineraries between Seoul and Beijing are illogical for some travelers. For example, what tourist would consider the path Seoul → Tokyo → Seoul → Beijing when they could go Seoul → Tokyo → Beijing? Going back to Seoul forms an unnecessary "loop", and it may be desirable to eliminate such *redundant paths* from the count as being irrelevant for this type of traveler. The word *redundant* is a technical term referring to paths containing loops (embedded cycles) and/or switchbacks (repeated edges). All such paths can be eliminated by calculating something called a *redundancy matrix*, denoted by R_N (where the subscript N indicates the number of legs, or edges, of a path and is equal to 3 in this case), which can then be subtracted from the path count provided by A^3 (A_p^3 in this example). What remains are non-redundant paths. Now, here is where things become tricky. Formulas exist for the direct computation of R_3 and R_4 from A , and even for R_5 and R_6 , although the formulas for these last two

redundancy matrices are very complicated.^{38,39} However, the real difficulty with all these formulas is that they only work when the entries of A are either 1 or 0.³⁸ In the case of flights connecting two cities, there will often be more than one round-trip connecting flight. Furthermore, the flight count may change from year to year, and with the seasons. So, rather than trying to develop closed form expressions for R_N that will quickly become obsolete as the connecting flight count between cities changes, an unpublished algorithm will be presented here that goes back to basics and employs combinatorics.

Calculations will begin with the direct computation of the individual elements of R_3 (R_{P_3} in this example). First of all, R_3 (i.e. R_{P_3}) has all zeros on its main diagonal. That is because only a *simple cycle* (no flight path reused) with no city (vertex) revisited (also called a *circuit* in the literature) can be made using 3 edges. In other words, there is no redundancy for a circuitual journey involving 3 legs (2-stops)! It is important to realize that in general this will not be the case for $N > 3$. Next, comes the computation of all the off-diagonal elements of the redundancy matrix. This is not as bad as one might think, because the redundancy matrix is symmetric! That is to say, any redundant path between two cities can also be followed in reverse. That symmetry cuts the number of calculations in half. Suppose the analyst wishes to calculate $R_{P_3}(2,3)$, representing all redundant paths between Beijing and Seoul that are 3 legs long. Clearly, by definition, the sequence of steps must begin with Beijing and end with Seoul (Beijing → X → Y → Seoul). But, what goes in between? If X is Seoul, then Y can be Beijing, Tokyo, Los Angeles, San Francisco, or Seattle; but not Seoul again because there are no flights from Seoul to itself. Suppose Y = Beijing, how many redundant paths exist? There are 6 paths from Beijing to Seoul (see Figures 3A and 6), and 6 more paths from Seoul back to Beijing, followed by another 6 paths to Seoul. That makes $6 \times 6 \times 6$, or 216 possible redundant paths. The other selections of Y yield 96, 24, 6, and 24 additional redundant paths respectively, for a sub-total of $216+96+24+6+24 = 366$ redundant paths. What if Y is fixed at Beijing? Then X can be

Tokyo, San Francisco, Seattle, or Los Angeles; but not Seoul because that has already been counted. The sub-total number of redundant paths produced by $Y = \text{Beijing}$ is $96+6+6+24 = 132$. Therefore, the

grand total is $366 + 132 = 498$ redundant paths. Therefore, $R_{P_3}(2,3) = 498 = R_{P_3}(3,2)$. Similarly, $R_{P_3}(1,6) = 225 = R_{P_3}(6,1)$, ... etc. The complete R_{P_3} matrix is displayed in Figure 9.

$$R_{P_3} = \begin{pmatrix} 0 & 364 & 376 & 144 & 138 & 225 \\ 364 & 0 & 498 & 84 & 81 & 178 \\ 376 & 498 & 0 & 168 & 84 & 184 \\ 144 & 84 & 168 & 0 & 126 & 159 \\ 138 & 81 & 84 & 126 & 0 & 150 \\ 225 & 178 & 184 & 159 & 150 & 0 \end{pmatrix} \quad F_{P_3} \equiv A_{P_3}^3 - R_{P_3} = \begin{pmatrix} 464 & 154 & 157 & 213 & 195 & 212 \\ 154 & 386 & 127 & 247 & 245 & 242 \\ 157 & 127 & 420 & 226 & 240 & 239 \\ 213 & 247 & 226 & 240 & 124 & 155 \\ 195 & 245 & 240 & 124 & 200 & 137 \\ 212 & 242 & 239 & 155 & 137 & 330 \end{pmatrix}$$

Figure 9 – The redundancy matrix R_{P_3} and the fundamental matrix F_{P_3} for Pacific Rim paths of length 3.

The difference between the matrix elements of $A_{P_3}^3$ and R_{P_3} yields the number of non-redundant paths between any two cities for paths that are 3 legs long (i.e. have two layovers). This new matrix will be called the *fundamental matrix for paths of length 3*, and will be denoted by $F_3(i,j)$, or $F_{P_3}(i,j)$ in this example, and is displayed in Figure 9. If $i \neq j$, these non-redundant paths are called *ways*. While the diagonal elements $F_{P_3}(i,i)$ yield the number of non-redundant cycles (called *circuits*), 3 legs long, that bring you back home to your starting city i . For example, the matrix element $F_{P_3}(5,5)$ is just the number of circuits 3 legs long that start from San Francisco and bring a traveler back to San Francisco. $F_{P_3}(5,5) = 200$, and there are indeed 200 non-redundant paths as the reader can verify. To avoid any confusion with the literature, the reader should note that there is a matrix called a *way matrix* $W_3(i,j)$, and for $i \neq j$ $W_3(i,j) = F_3(i,j)$, but for all $i = j$ $W_3(i,i) \equiv 0$; so, the way matrix contains only ways (paths for which no edge or vertex is revisited), while

the fundamental matrix contains both ways and circuits (paths for which no edge is revisited, but the first and last vertex are identical). At this point the reader may wonder if there is an independent method for cross checking the entries of F_{P_3} ? Yes, there is!

Continuing with the example above involving travel between Beijing and Seoul, the matrix element $F_{P_3}(2,3)$ indicates that 127 non-redundant (simple) paths exist between these two cities. These paths can be counted directly without subtracting the number of redundant paths from the total number of paths. Again, by definition, the sequence of non-redundant paths must begin with Beijing and end with Seoul (Beijing $\rightarrow X \rightarrow Y \rightarrow$ Seoul). Between these two endpoints there are two cities, and it is necessary to calculate the number of paths for all *permutations* of those cities. There are “4 chose 2” such permutations, or $4! / (4 - 2)! = 12$ permutations, and they are:

| | | |
|--|---|------------------------|
| $4 \times 3 \times 2$ Beijing \rightarrow Tokyo \rightarrow Los Angeles \rightarrow Seoul | = | 24 non-redundant paths |
| $4 \times 2 \times 1$ Beijing \rightarrow Tokyo \rightarrow San Francisco \rightarrow Seoul | = | 8 non-redundant paths |
| $4 \times 2 \times 2$ Beijing \rightarrow Tokyo \rightarrow Seattle \rightarrow Seoul | = | 16 non-redundant paths |
| $2 \times 3 \times 4$ Beijing \rightarrow Los Angeles \rightarrow Tokyo \rightarrow Seoul | = | 24 non-redundant paths |
| $1 \times 2 \times 4$ Beijing \rightarrow San Francisco \rightarrow Tokyo \rightarrow Seoul | = | 8 non-redundant paths |

| | | |
|--|---|-------------------------------------|
| 1 × 2 × 4 Beijing → Seattle → Tokyo → Seoul | = | 8 non-redundant paths |
| 2 × 3 × 1 Beijing → Los Angeles → San Francisco → Seoul | = | 6 non-redundant paths |
| 1 × 3 × 2 Beijing → San Francisco → Los Angeles → Seoul | = | 6 non-redundant paths |
| 1 × 3 × 2 Beijing → Seattle → Los Angeles → Seoul | = | 6 non-redundant paths |
| 1 × 3 × 1 Beijing → Seattle → San Francisco → Seoul | = | 3 non-redundant paths |
| 1 × 3 × 2 Beijing → San Francisco → Seattle → Seoul | = | 6 non-redundant paths |
| 2 × 3 × 2 Beijing → Los Angeles → Seattle → Seoul | = | 12 non-redundant paths |
| | | <hr/> 127 total non-redundant paths |

There are no other permutations. Therefore, the total number of non-redundant paths is 127, in agreement with the value of $F_{P_3}(2,3)$ computed by subtracting the redundancy matrix from the adjacency matrix cubed. So, the analyst can be quite sure that all the arithmetic has been done correctly. Note that there are also 12 permutations for journeys that start from San Francisco and return to San Francisco in 3 legs (2 layovers) and, if all the arithmetic is done correctly, the total number of non-redundant paths (circuits) will be 200, the value of the matrix element $F_{P_3}(5,5)$.

The next question is, "What about paths that are 4 flights long, involve 5 cities, and have 3 layovers? How many paths do they generate?" In this case it is best to generate the matrix elements of the fundamental matrix directly. Again, consider traveling from Beijing to Seoul (Beijing → X → Y → Z → Seoul). Since Beijing and Seoul have already been used as the first and last cities, X, Y, and Z can only be Tokyo, San Francisco, Seattle, or Los Angeles. How many ways can X, Y, and Z be selected from these 4 cities. The answer is $4!/(4-3)! = 4!/1! = 4! / 1 = 4 \times 3 \times 2 \times 1 = 24$ permutations. Although there are now twice as many permutations, the matrix elements of F_{P_4} , the total number of non-redundant paths (ways) and circuits 4 legs long, can still be calculated manually as in the previous paragraph for F_{P_3} . If the

number of redundant paths is of interest, these can be easily obtained by subtracting F_{P_4} from A_P^4 .

What about paths 5 flights long (e.g. Beijing → W → X → Y → Z → Seoul). Business travelers might do something like this. Now the number of permutations is $4!/(4-4)! = 4!/0! = 4!/1 = 4! = 24$ again. If even longer journeys are contemplated, there aren't enough cities to guarantee the existence of a non-redundant path.

The diagonal elements of $F_N(i,i)$, regardless of whether the fundamental matrix applies to the North Atlantic, the Pacific Rim, or the globe, are of special interest because most travelers eventually want to return home following a simple circuit without revisiting cities. The sum of all the diagonal elements yields all possible circuits of length N (N flights). This sum is called the *trace* of F_N , and is denoted by $tr(F_N)$. Whatever the regional or global flight schedule is between cities, the larger the trace, the greater the risk of spreading an infection for circuits of length N. For a region with 6 major cities, N can be no greater than 6. Therefore, the total infection risk R_T is proportional to a sum over N, viz.

$$\mathcal{R}_T \propto \text{tr}(A^2) + \text{tr}(F_3) + \text{tr}(F_4) + \text{tr}(F_5) + \text{tr}(F_6) = \text{tr}(A^2) + \sum_{N=3}^{N=6} \text{tr}(F_N) , \quad (1)$$

where the upper limit on the summation over N will, in general, be one less than the number of cities considered.

Reduction of the notion of risk to a single proportionality for regional or global air travel is an important result because it allows the analyst to select the safest flight network among a set of such networks. As a simple example, consider Pacific Rim circuits that are two and three edges long. These are some of the most common cycles for travelers. In that case equation 1 can be truncated after the second term. From Figures 7 and 9, $\mathcal{R}_T \propto \text{tr}(A^2) + \text{tr}(F_3) = 254 + 2040 = 2294$. Now suppose that one flight of the critical route between Beijing and Seoul is cancelled. In that case, since the resulting network is just a sub-graph of the original, it must possess a total infection risk smaller than the original network, call it \mathcal{R}'_T . Repeating the calculations above, and noting that only the diagonal elements $A_p'^2(i,i)$ and $F'_{p3}(i,i)$ of the sub-graph are required, yields $\mathcal{R}'_T \propto 232 + 1902 = 2134$, a smaller value for the infection risk ($\mathcal{R}'_T < \mathcal{R}_T$), as would be expected. However, the 7.0% decrease in infection risk (via a decrease in the number of travel circuits) has been achieved by cancelling just one flight between Beijing and Seoul in this very infection sensitive part of the world. Cancelling one flight is equivalent to decreasing the total number of flights for the whole network by only 2.6%; where the total number of flights is the sum of the matrix elements above (or below) the main diagonal of A_p , i.e. $\sum_i \sum_j A_p(i,j)$ for all $j > i$. *Therefore, surprisingly, the spread of infections can be decreased significantly with negligible decreases in passenger through-put by prudent scheduling changes.* Now, what would happen if an extra nonstop flight from Beijing to Los Angeles were added, while a nonstop flight from Tokyo to Los Angeles is eliminated? Now which network is most resistant to the spread of disease? Clearly, equation 1, or some similar metric for \mathcal{R}_T , that depends on the matrix elements of A^N ,

\mathcal{R}_N , and/or F_N is required to answer such questions objectively. The number of such rules being limited only by human imagination and the requirements of the specific problem to be addressed.

The bottom line of this discussion on matrix methods is that the adjacency, redundancy, and fundamental matrices are powerful tools. They can be used to identify risky travel behavior and risky airline scheduling. They can also be used to identify cities where infections are likely to be observed first during the early stages of a pandemic. As everyone knows from the economic and social difficulties of the “lockdown”, *even during a pandemic, life must go on!* Some travel is inevitable, but flight schedules and travel behavior can be modified to mitigate the risk of spreading infection. Furthermore, genomic surveillance in “early warning” cities like Seoul and London, tells governments and airlines when it is time to initiate changes. Although matrix methods are well suited for calculating the risk of spreading disease via air travel (Fig. 2 black lines - solid, dashed, and dotted), they don’t tell us everything we would like to know about the spread of disease. As Figure 2 shows, there are other factors to consider – population migration, both legal and illegal (Figure 2 arrows in black outline), and the circulation of disease (Figure 2 curved gray arrows). The description of that part of the COVID story will require very different tools – the mathematics of chaos, and unstable sets of non-linear differential equations.

The Current Human Diaspora

The Southern Hemisphere and the parts of the Northern Hemisphere south of the U.S. and Europe were an important source of COVID vectors. In the Western Hemisphere (Figure 2) the migration of human populations, especially undocumented (illegal) aliens, through America’s porous southern border introduced millions of people into the U.S. whose health status was unknown.⁴⁰ However, testing of

individuals who were arrested by U.S. Customs and Border Protection as they attempted the crossing, indicated that during the peak COVID years (2021 and 2022) about one-third were infected by the time they reached the border.^{40, 41, 42} Most of these migrants come from Mexico, the Central American states, and heavily infected South America. Some come from even further away. Fleeing war, drug related violence, and poverty, they enter South or Central America first, and then travel north.

In Europe (Figure 2), Spain, Italy, and Greece, were on the “front-lines” of the immigration surges from Africa, the Middle East, and Asia in general. Resentment was high. In Sicily, the local people would say, “*Compra, Morta*” (“you buy, you die”) – a reference to the fact that many migrants who entered Italy along the South Africa-Tunisia-Pantelleria Is.-Sicily migration route end up as street peddlers in Sicilian cities. In Spain the passage from all of Africa, through Morocco, across the Strait of Gibraltar, and into Spain is another obvious migration route into the European Union (EU). However, “*eme-once*” (“*M-11*”) – referring to the March 11, 2004 jihadist terrorist attack in which 10 simultaneous explosions on four commuter trains in Madrid killed 191 people and injured more than 1,800 others – left a negative impression of Muslim North African (*magreb*) migrants in the mind of many Spaniards, especially in Madrid. It was the worst terrorist attack in European history, and is still recognized as a day of mourning 20 years later in Spain.⁴³ Some Spaniards will talk about it, but most are hesitant to express their feelings to people they don’t know. Finally, Greece has become another gateway into the EU. Middle Easterners, Africans, and Asians make their way through Turkey into Greece and beyond. Migration had already reached the 1 million mark by 2015. Many make their way to the Greek islands, but thousands have died at sea in the attempt. The recent fighting in Gaza has seen a 400% increase in migration into Greece in the February to March 2024 time-frame.⁴⁴ Although France is not on a direct migration route into Europe, it has experienced a significant African immigration that is most obvious in the suburbs south of Paris (e.g., from

Parc Médicis to *Le Delta* in the *Rungis* neighborhood). In the next section, the consequences of African migration into Europe will be brought into sharper focus.

The Chaotic Behavior of Epidemics/Pandemics

Some Questions: Diversity analysis suggests that the appearance of omicron BA.2.86 in Israel and Denmark originated in South Africa together with the other omicron strains BA.1 through BA.5.⁴⁵ Therefore, it seems likely, or at least plausible, that the migration route through the Middle East may have been instrumental in the spread of BA.2.86 into Israel (one of the black arrows in Figure 2), while air travel may have been involved for the spread into Denmark (see air-route maps – Figure 1 of reference 45). Graeme Dor and his colleagues raise the following interesting question, “How is it possible that ‘despite its relative remoteness and the fact that it is home to only 0.7% of the world’s population, South Africa has had a disproportionately large impact on SARS-CoV-2 evolution and spread?’”⁴⁵ Still more surprising is that the beta-strain also originated in South Africa! The short answer to the question raised by Dor et al. is that the omicron strains simply “out-competed” beta and the other strains. What, however, does that actually mean for a virus? – A question that will be answered immediately.

Initial Growth (A Simple Discrete Model): Let MICLP be the *Mean Incubation Carrier Latency Period*, during which each vector attempts to infect m other people; a period of about 5 days before symptoms and isolation. Furthermore, let \mathbf{n}_0 be the initial number of infected people in a population of size \mathcal{N} , and let \mathbf{n}_p be the number of infected people after p MICLP time periods, where p is an integer. Define the growth rate r as the mean relative increase per MICLP:

$$r \equiv (\mathbf{n}_{p+1} - \mathbf{n}_p) / \mathbf{n}_p, \text{ where } r > 0. \quad (2)$$

Therefore, $\mathbf{n}_{p+1} = (r + 1) \mathbf{n}_p$. (3)

Therefore, if r is constant, $\mathbf{n}_p = (r + 1)^p \mathbf{n}_0$. (4)

Alternately, if t is the total time elapsed from the start of an infection measured in days, then a dimensionless time measure τ can be defined such that $\tau \equiv t/\text{MICLP}$. Therefore, by the definition of m ,

$$\mathfrak{N}_p = \mathfrak{N}_0 m^\tau, \quad (5)$$

where τ may be rounded off to make it an integer like p . Comparing equations 4 and 5 yields $m = r + 1$, or $r = m - 1$. This simple, but important, result means that the viral strain with the largest m will have the largest mean relative increase per MICLP, and will out compete all other strains. For the alpha strain, $m \approx 3$ and $r \approx 2$. Therefore, the delta strain has $-6 \leq m \leq -12$ and $-5 \leq r \leq -11$. For omicron, $-15 \leq m \leq -45.6$ and $-14 \leq r \leq -44.6$.³⁵ Here, the symbol “~” means “approximately”, while “ \approx ” means “approximately equal to”. These figures for m and r will be of great value for the calculations that follow.

Steady State Behavior and the Frontier of Chaos (The Discrete Verhulst Model for an isolated population): Obviously, the growth in equation 5 cannot continue forever because susceptible individuals will be consumed by either death or the development of natural immunity upon recovery. Artificial vaccination will also speed the development of herd immunity. While the warm summer months can retard the growth of respiratory infections. Finally, a strain can die out because it is replaced (out-competed) by a new strain with an even larger m , as previously discussed. Eventually, the number of active cases must level off. A good example of leveling behavior due to these factors is offered by the first and second waves of COVID in the U.S. prior to September 26, 2020.³⁵ If population immunity continues to grow, the number of cases per day will eventually crash. An example of this was the abrupt drop in the number of active cases in the U.S. following the omicron peak.³⁵ Here, Verhulst dynamics will be used to model observed leveling behavior.⁴⁶ It will be assumed that equation 2 is replaced by

$$r(1 - [\mathfrak{N}_p / \mathfrak{N}_{\max}]) = (\mathfrak{N}_{p+1} - \mathfrak{N}_p) / \mathfrak{N}_p, \quad (6)$$

where \mathfrak{N}_{\max} is the limiting (maximum) number of active cases. That is to say, the left side of equation

2 is no longer just a constant r , but approaches zero as $\mathfrak{N}_p \rightarrow \mathfrak{N}_{\max}$ and $p \rightarrow \infty$. It is important to remember that equation 6 is just a model that mimics the behavior of a much more complex process, and is not the process itself. Notice also that both sides of equation 6 are dimensionless. That is a significant point that will be revisited in the next section. Equation 6 can be rewritten as

$$\mathfrak{N}_{p+1} = r \mathfrak{N}_p - r (\mathfrak{N}_p^2 / \mathfrak{N}_{\max}) + \mathfrak{N}_p. \quad (7)$$

Since \mathfrak{N}_{\max} can be anything, equation 7 will be normalized by dividing it by \mathfrak{N}_{\max} to facilitate calculations. Therefore, equation 7 becomes

$$\underline{\mathfrak{N}}_{p+1} = r \underline{\mathfrak{N}}_p - r \underline{\mathfrak{N}}_p^2 + \underline{\mathfrak{N}}_p, \quad (8)$$

where $\underline{\mathfrak{N}}_{p+1} \equiv \mathfrak{N}_{p+1} / \mathfrak{N}_{\max}$, and $\underline{\mathfrak{N}}_p \equiv \mathfrak{N}_p / \mathfrak{N}_{\max}$. Equation 8 can now be rewritten as

$$\underline{\mathfrak{N}}_{p+1} = (r + 1) \underline{\mathfrak{N}}_p - r \underline{\mathfrak{N}}_p^2, \text{ where } r > 0. \quad (9)$$

Dimensionless equation 9 allows the *subcritical*, *critical*, and *supercritical* behavior of the Verhulst model to be studied. Figure 10 shows what happens to $\underline{\mathfrak{N}}_p$ as $p \rightarrow \infty$ for various values of r , starting from an initial value $\mathfrak{N}_0 = 0.1$. Note that $\mathfrak{N}_0 \neq 0$, because $\mathfrak{N}_0 = 0$ means there is no disease to start with. Therefore, a truly isolated population will have no disease in the future. Therefore, $\underline{\mathfrak{N}}_{p+1}$ will also equal zero, as can be verified by inspection of equation 9.

Starting with a subcritical value of $r = 1.9$, $\underline{\mathfrak{N}}_p$ overshoots at first, then undershoots, and then eventually settles down to the steady state value of unity. This was happening during the third COVID wave in the U.S. before its oscillations were cut off by the growth of the delta wave.³⁵ The damped oscillatory behavior can be better understood if the departures of $\underline{\mathfrak{N}}_p$ from unity (call them δ_p) are tracked as $p \rightarrow \infty$. Let $\underline{\mathfrak{N}}_p = 1 - \delta_p$, then $\underline{\mathfrak{N}}_{p+1} = 1 - \delta_{p+1}$. Substituting these values for $\underline{\mathfrak{N}}_p$ and $\underline{\mathfrak{N}}_{p+1}$ into equation 9 yields

$$1 - \delta_{p+1} = (r + 1)(1 - \delta_p) - r(1 - \delta_p)^2. \quad (10)$$

Expanding, ignoring the terms of negligible size in δ_p^2 , and recollecting, yields

$$\delta_{p+1} \approx (1 - r) \delta_p. \quad (11)$$

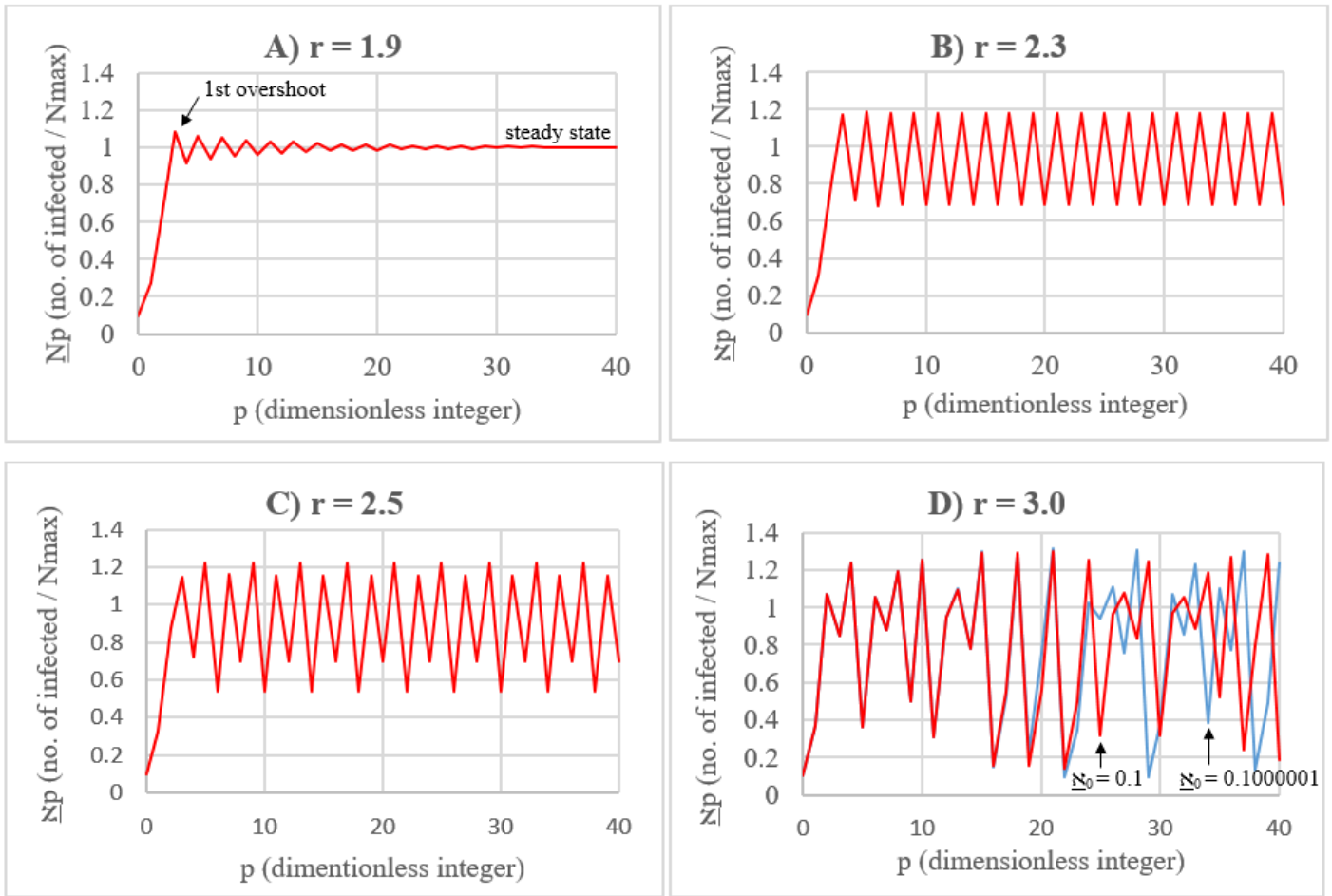


Figure 10 – The evolution of \underline{x}_p as a function of p for various values of r . A) $r = 1.9$ (subcritical / well-behaved). B) $r = 2.3$ (late sub-critical). C) $r = 2.5$ (near the frontier of chaos). D) $r = 3$ (supercritical / chaotic). All graphs used $\underline{x}_0 = 0.1$, but the numerical values in blue for the chaotic process in D are associated with $\underline{x}_0 = 0.1000001$. If $\underline{x}_0 = 0.100000001$ then the blue and red curves again lose synchronicity, but it is later regained over $0 < p \leq 40$.

This simple approximation shows that there is no overshoot when $0 < r \leq 1$, because the departures δ_p form a monotonically decreasing series, or 0 if $r = 1$. Above $r = 1$, overshoot grows as $r \rightarrow 2$. At $r = 1.9$, $\delta_{p+1} = -0.9 \delta_p$. Therefore, the deviations *alternate in sign* and decrease in magnitude as $p \rightarrow \infty$ and $\underline{x}_p \rightarrow 1$. For $r \geq 2$, approximation 11 predicts that $|\delta_{p+1}| \geq |\delta_p|$. Therefore, the steady state value of $\underline{x}_p \rightarrow 1$ is no longer attainable as $p \rightarrow \infty$.

For example, if $r = 2.3$, the Verhulst model begins to show critical behavior, as \underline{x}_p oscillates between two values as $p \rightarrow \infty$; one value at $\underline{x}_p \approx 1.18$, and the other at $\underline{x}_p \approx 0.69$, such that the old steady state at $\underline{x}_p = 1$ is asymmetrically bracketed. So long as $2 < r < \sqrt{6} \approx 2.449$, only two stable values of \underline{x}_p will exist. Although the alpha strain was first detected in the U.S. in November 2020, it did not become dominant until March 2021. The first two COVID waves in the

U.S. each achieved a stable number of active cases, and were primarily the original SARS-CoV-2 strain; something close to B.1 that is sometimes called L.³⁵ At $r = 2.5$, four steady state values appear. When $r > 2.570$ (called the *critical value*, r_c), chaotic behavior sets in (see Figure 10D for $r = 3$), and the value of \underline{x}_p appears to fluctuate randomly around the original steady state value $\underline{x}_p = 1$ (called a *strange attractor*), but *within bounds*. This behavior is what might be expected for the delta and omicron strains, making it very difficult to predict the future number of active cases, or the amount of medical supplies that will be required. Another chaotic behavior is the variable number of integers (proportional to time) between deep troughs; it's like the variable duration of "annual" COVID cycles.³⁵

It is significant that the behavior of the Verhulst model is very sensitive to the value of r near 2.570,

with small changes resulting in the multiplication of steady states. Figure 11 shows the splitting (or *bifurcation*) diagram for the number of steady states as a function of r for this system. This curious diagram contains an infinite number of “holes”, like a thin piece of Swiss cheese with an infinite number of holes of various sizes. If a vertical cut through this diagram is made at $r_c = 2.570$ (red dashed vertical line in Figure 11), at no point will it be a truly continuous one-dimensional line, even though its points mark off an infinite number of states! Such a cut has a dimension that is less than one. Its *Feigenbaum dimension* is 0.538 – it is *fractionally dimensioned*, and it is for this reason that the bifurcation diagram is called a *fractal*. Stranger still, Figure 11 possesses a property of self-similarity in the sense that a microscopic piece of the diagram is a copy of the whole! It is also significant that the chaotic

behavior of the Verhulst Model is *very* sensitive to initial conditions. If $\underline{x}_0 = 0.1000001$ instead of 0.1, a change of only one part in a million, Figure 10D shows (blue) that after 19 iterations the values of \underline{x}_p will begin to diverge from the original values (red). After 40 iterations the calculated values of \underline{x}_p are completely out of phase with one another. Therefore, the introduction of even a single new COVID case involving a strain with sufficiently large r (and therefore m) into an isolated, but previously infected, population can completely change the future course of a pandemic in that population. This phenomenon is called the “butterfly effect” for reasons that will be discussed presently. It’s an unpleasant answer to the question raised by Dor and, as will be demonstrated in the next section, the situation is exacerbated when people travel.

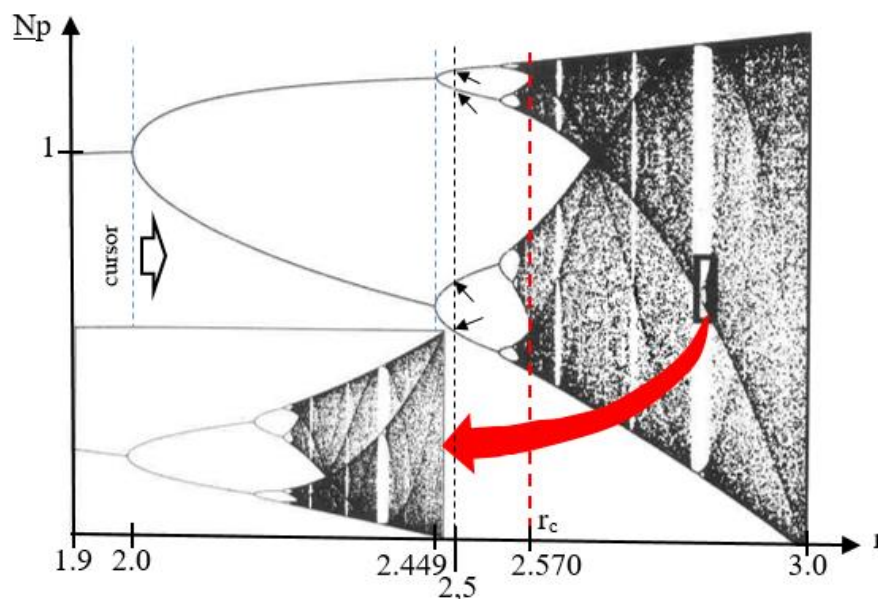


Figure 11 – The splitting diagram for steady states as a function of r . The insert is a magnified view of a small part of the main diagram enclosed within the black box. At $r = 2.5$, N_p oscillates between 4 values marked by small arrows. At $r = r_c = 2.570$ there are an infinite number of possible steady states – chaotic behavior!

The Infection-Convection Analogue (An Analytic Model for Circulating Populations)

The use of system analogy is a well-established principle of engineering that forms the foundation of systems analysis. For example, an electrical inductor

is analogous to a mechanical spring, a resistor is analogous to a mechanical viscose damper, and a capacitor is analogous to a mass.⁴⁷ The word “analogous” in this context means that the behavior of the corresponding electrical and mechanical elements (the electro-mechanical analogues) can be described by equations with a similar form. In

this section, the spread of disease over the surface of the earth will be modeled as two-dimensional convection in a vertical slab of fluid heated from the bottom. Such a physical process is governed by the Lorenz equations⁴⁸ – a coupled set of three non-linear differential equations that have been used to model the behavior of lasers, dynamos, chemical reactions, and electric circuits.^{49,50,51,52} The Lorenz model also seems particularly applicable for describing the circulation of infected people (vectors) between neighboring countries in Eurasia and North America, or over the Atlantic and Pacific flight paths. People are neither created nor destroyed during these circulations in the same way that mass is neither created nor destroyed during the convection circulation of an *approximately incompressible fluid*. Therefore, the population between “neighboring” states (in a geographical or flight sense) remains the same – *on the average*. Therefore, neighboring states form an infection *convection cell*. The source of “heat” for this cell are the infected people in the source country. As “hot” infected people leave the source, “cold” uninfected (or relatively uninfected) people from the target (uninfected, or relatively uninfected) country replace those who left the source – *on the average, because in the end everyone must return to their nation of origin*. This process is, of course, analogous to the physical convection process where low density hot fluid rises while cold dense fluid sinks to replace it, and gravity supplies the driving force for the circulation of mass. In the case of an epidemic on a local scale, or a pandemic on a global scale, it is the concentration gradient of infected people that supplies the driving “force” for the spread of infection, just as a molecular concentration gradient supplies the driving “force” for the diffusion of molecules in chemistry (the *chemical potential*).

Continuing with this infection-convection analogy, let I be a dimensionless variable proportional to convective intensity normally measured in watts of heat transferred, or the number of people leaving a source country per MICLP. Furthermore, let ΔT be a dimensionless variable proportional to the

temperature difference between the ascending and descending currents during fluid convection, or the difference in the number of vectors between departing and returning travelers per MICLP (call it ΔS). Finally, let D be a dimensionless variable proportional to the distortion of the vertical temperature profile from linearity, such that a positive value indicates that the strongest gradients occur near the upper and lower fluid boundaries while a negative value of D indicates the reverse. Or, from an epidemiological point of view, D represents departure in the number of vectors from a linear gradient that has a large number of infected people in the source country and a small number of infected in the target country. In terms of these dimensionless variables, the coupled Lorenz equations, a set of equations that *approximately* describes convection, can be written as

$$\begin{aligned} dI/d\tau &= \sigma(\Delta T - I) \\ d\Delta T/d\tau &= I(\rho - D) - \Delta T \\ dD/d\tau &= I\Delta T - \beta D \end{aligned} \quad (12)$$

where the derivatives $dI/d\tau$, $d\Delta T/d\tau$, $dD/d\tau$, are simply the change in I , ΔT , and D with respect to τ , a dimensionless time measure used in fluid mechanics. For epidemiological purposes, τ will simply be the time measured in dimensionless MICLP units (i.e. $\tau \equiv t/\text{MICLP}$). Here, it is important to note that equations 12 are *dimensionless*, just like equations 6 and 9 above. In fluid mechanics, the dimensionless constants σ , ρ , and β , are the Prandtl number (the ratio of fluid dynamic viscosity to thermal conductivity, multiplied by the constant specific heat capacity to make the ratio dimensionless), the Rayleigh number divided by a critical constant (a measure of fluid layer turbulent instability), and a geometric factor related to the aspect ratio of a convection cell, respectively. For this report the interpretation of β remains the same for the infection convection cell, and the Saltzman/Lorenz value of 8/3 will be retained.⁴⁸ The infection convection cell is much larger than a two-dimensional fluid convection cell, but the ratio of its length to its width will be taken as constant. Furthermore, ρ is still a measure of instability in the

sense that the more infectious a disease is (the larger it's value of m), the more likely it is that the infection will spread in a "turbulent" and unpredictable way (i.e. ρ is a function of m , $\rho = f(m)$). Here ρ is analogous to r in equation 9, and the Saltzman/Lorenz value of $\rho = 28$ seems a reasonable model for omicron.⁴⁸ Finally, travel is not instantaneous. There are schedules that cannot be exceeded, layovers, delays, passenger limitations on flights, etc. All of these obstacles form a kind of travel "viscosity", or speaking electro-mechanically, they constitute "resistance" or "viscose damping". While thermal conductivity (the diffusion of heat) is analogous to the slow diffusional spread of infection without traveling (i.e. neighbor to neighbor transmission). So, the Prandtl number (σ), a measure of the relative importance of viscose to thermal effects, can be interpreted epidemiologically, and the analogy between fluid convection and the spread of disease is complete. For a compressible gas like air $\sigma < 1$, but for an almost incompressible fluid like water $\sigma = 7.56$. It is this latter incompressible case that applies to the spread of disease. Therefore, the Saltzman/Lorenz value of $\sigma = 10$ seems reasonable when modeling the circulation of disease vectors.⁴⁸

The solution to the system of equations 12 is well known,⁴⁸ and is presented graphically in Figure 12 for $\sigma = 10$, $\rho = 28$, and $\beta = 8/3$. Each point on the curve represents a solution to equations 12 at a particular point in time. As dimensionless time τ progresses, the curve evolves and orbits around two centers (C and C') chaotically, flipping back and forth between the two, but remaining confined to a bounded region of $I, \Delta T, D$ space.⁵³ Notice that I

can be negative, meaning that flow in the convection cell has reversed. So long as I and ΔT have the same sign warm fluid is ascending and cold fluid is descending. The opposite is true for positive I and negative ΔT . Such a phenomenon is physically possible momentarily if too much heat is added to the bottom of a vertical two-dimensional fluid system so that convective circulation becomes chaotic, thereby allowing for random flow reversals.⁵⁴ By analogy, if the current of travelers exceeds the capacity of the target nation's port of entry, an infection can "back-up" into the source nation. Similar conditions were met along the U.S./Mexico border during the pandemic as migrants waiting to enter the U.S. accumulated in border cities like San Luis Rio Colorado, Agua Prieta, and Nogales, Mexico; to be discussed in more detail in the next section. *Epidemiologically, chaotic behavior means that it is impossible to predict the future course of an outbreak of any highly infectious disease ($\rho \gg 1$) beyond setting broad limits on infection levels.* It's like trying to make accurate long-term predictions about the weather in a convective atmosphere!

Each center (C and C') in Figure 12 is a strange attractor, and represents a stable solution to equations 12. That is to say, steady state convection for either the spread of disease, or the spread of heat by convection in a vertical fluid slab. The $I, \Delta T, D$ coordinates of these strange attractors are easy to calculate because stable convection means $dI/d\tau = d\Delta T/d\tau = dD/d\tau = 0$. Therefore, equations 12 become

$$\sigma(\Delta T - I) = 0, \quad I(\rho - D) - \Delta T = 0, \quad \text{and} \quad I\Delta T - \beta D = 0. \quad (13)$$

Solving this new system of equations by simple algebra yields $I = \Delta T = \pm \sqrt{\beta[\rho - 1]}$ and $D = \rho - 1$. Substituting in the values of the dimensionless constants yields $D = 27$ and $I = \Delta T = \pm 6\sqrt{2} \approx \pm 8.485$, as can be seen in Figure 12. Note that no convection at all corresponds to the solution $I = \Delta T = D = 0$.

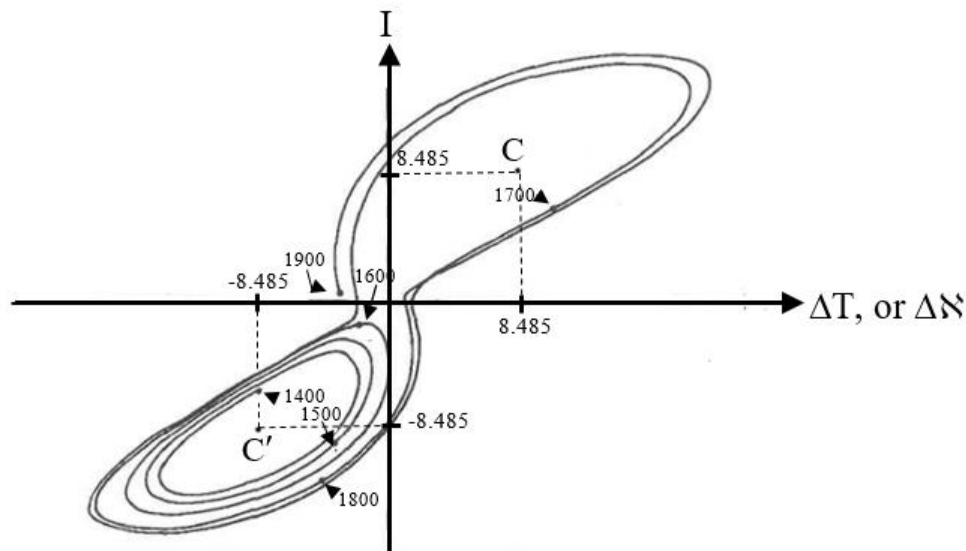


Figure 12 – A solution to Equations 12, projected onto the I - ΔT plane, as a function of time for $\sigma = 10$, $\rho = 28$, and $\beta = 8/3$. C and C' are steady state strange attractor centers. Digital integration used dimensionless time increments $\Delta\tau = 0.01$, and began from a state $(I_0, \Delta T_0, D_0) = (0, 1, 0)$ that departs slightly from no convection (i.e. $I = \Delta T = D = 0$). This translates to a small imbalance in the number of active cases between two neighboring countries. The numbers on the trajectory extend from 1400 to 1900 iterations. Notice that the solution initially “overshoots” and tries to escape from attractor C' . It is then caught by attractor C , only to return to C' at the end of its trajectory. Note also that the period of each orbit varies as τ progresses (i.e. the intensity, direction, and *duration* of reversals are all unpredictable). Chaotic flow reversals of this kind are unique to the Lorenz model and have no counterpart in Verhulst dynamics.

The onset of the chaotic behavior just described is largely determined by ρ . If the values of σ and β remain constant at 10 and $8/3$, respectively, unstable chaotic behavior will begin at the critical value $\rho_c = 470/19 \approx 24.74$. Values of ρ above ρ_c are called *supercritical* (as in the previous section), those below are called *subcritical*; and, of course, ρ_c is analogous to the Verhulst r_c . Subcritical solutions to equations 12 are well behaved and orbit around either the C or C' strange attractor when $1 < \rho < \rho_c$. That is to say, convection of fluid mass, or disease vectors, will oscillate in $I, \Delta T, D$ space around one attractor in a predictable way until $I, \Delta T$, and D , settle down to that steady state attractor value. Small changes in ρ near ρ_c can affect the behavior of the solutions to equation 12 dramatically, as in Figure 10 for the more easily understandable Verhulst model. In addition, like the Verhulst model, the Lorenz model also displays sensitivity to initial conditions. Any small change to the starting values $I_0, \Delta T_0$, and D_0 in figure 12 will be amplified over time so that after a sufficiently long period, the final values of $I, \Delta T$, and D will be completely different. That is to say, a small

change to the initial state of the system does not result in a small change to the final state. This is the “butterfly effect” of the Verhulst model – referring to the idea that even the flapping of a butterfly’s wings can change the weather in a convective atmosphere far enough into the future. Once again, even a single case of beta, or omicron, in a remote, underpopulated location like S. Africa, has global implications if enough time has passed. Dr. Tlaleng Mofokeng of South Africa was quite right to be concerned about the lack of COVID vaccine in Africa.⁵⁵ The result of this neglect was calamitous! *In the future, it would be wise to establish regional stock piles of vaccines and other medical supplies from the very beginning of an outbreak, on a regional population basis, to prevent this type of imbalance from occurring again.*

Although the calculations of the previous two sections explain many of the observed behaviors of the COVID-19 pandemic, all models have their limitations, and these must be addressed before closing this section. It has been tacitly assumed that for convection in a vertical slab of fluid, the

temperatures at the top and bottom of the slab remain constant. However, in most closed systems, the fluid will eventually heat up, unless some special provision is made to prevent that from occurring. The same is true during a pandemic as a highly infected country slowly spreads disease to its neighbor. Therefore, the infection-convection model cannot be run for too long, and must be confined to a narrow window in dimensionless time τ , as in Figure 12. Another obvious limitation is that the behaviors of the Verhulst and Lorenz models apply to a single strain with fixed m . When multiple strains are present either simultaneously, or separated in time, behaviors might overlap in a complex way that is outside of the descriptions presented here.

Lessons Learned from Around the Globe (traveling west from the U.S.)

Southwestern U.S. / Northwestern Mexico: Although the U.S. southern border was theoretically closed, the reality was a porous border through which millions of migrants passed. In 2021 (the year of the delta wave) 1.4 million people tried to illegally cross the U.S./Mexico border, and in 2022 (the year of the omicron wave) 2.4 million tried to cross the border.⁵⁶ Many of these migrants remained in the U.S. by legal device and lengthy court proceedings. Of the 3.8 million that were intercepted in 2021 and 2022, one third were sick by the time they reached the U.S. border.^{41,42} However, the intercepted migrants comprise only a fraction of total illegal migration. It has been estimated that about 11.8 million “unauthorized immigrants” live in the U.S. as of Aug. 2025.⁵⁷ In addition, *legal* immigration proceeded at a brisk pace during 2021 and 2022 with about 1.5 and 2.6 million entering the U.S. respectively; an average of 341,666 people per month over this two-year period.⁵⁸ Health checks must have been few if any, since, on the average, 1.3 people entered the U.S. every 10 seconds! In Nogales, Arizona, the chain of people entering and leaving the border station was often continuous. However, the damage didn't stop there. During the first week of September 2024, in Phoenix, Arizona, the author witnessed

migrants being transported, in a new cross-country bus from a large 4+ star hotel near the intersection of Interstate Highway 10 and Baseline Road, to other parts of the U.S. Each had spent the previous night at the hotel, was fed breakfast in the morning, and given a new cell phone for their journey. Nothing more could have been done to spread COVID! Figure 13 summarized the result. The message is quite clear. The U.S. southern border from San Diego, California, to Corpus Christy, Texas, had become heavily infected, as migrants buried themselves in densely populated border metropolises, or sought work in agricultural areas. And what was the U.S. CDC's reaction to these irresponsible, bizarre, and suicidal policies? – *Absolute Silence!* How can anyone wonder why the U.S. had more COVID cases than any other country in the world?

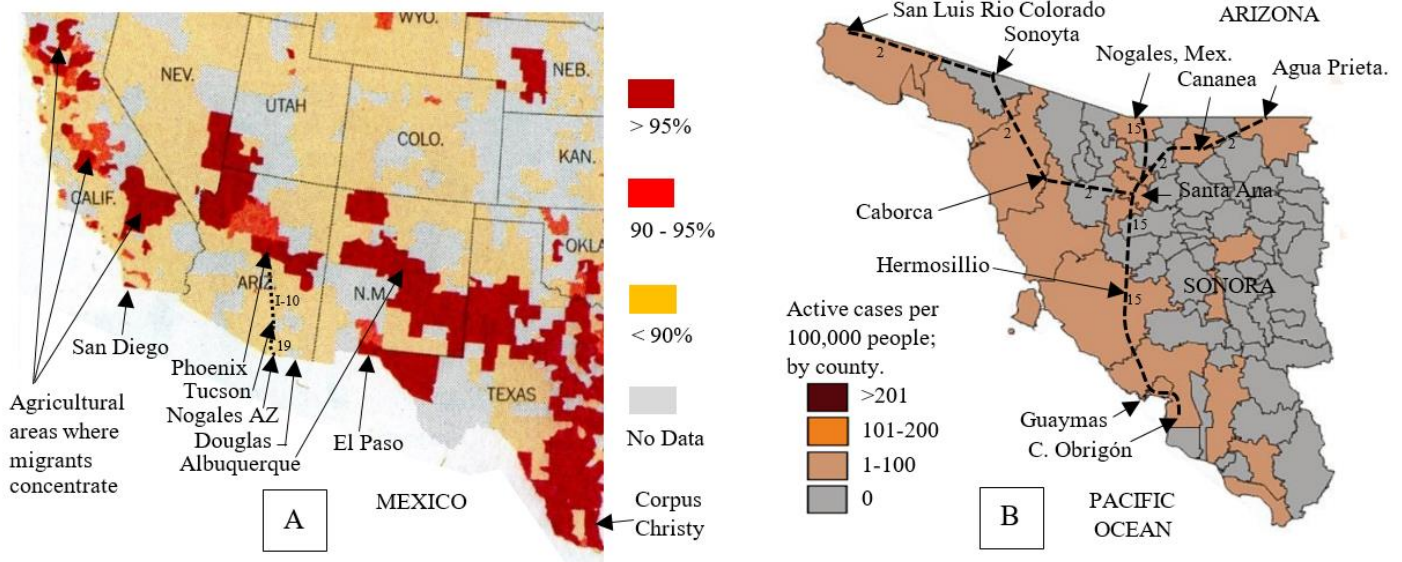


Figure 13 – A) Share of Intensive Care Unit (I.C.U.) beds occupied in each hospital service area. For the week ending Sept. 9, 2021 – the Delta Wave.⁵⁹ Map cropped, enlarged, and annotated by the author. The number of infections was so massive that many counties were simply running out of beds for the critically ill! B) Active cases per 100,000 people in Sonora Mexico. Map dated May 16, 2022 and updated weekly.⁶⁰ Actual case count may be much higher because only 10,503,678 tests were administered nationally as of Oct. 15, 2021, vs. 929,349,291 tests in the U.S. as of July 29,2022.⁶¹ Dotted lines with highway numbers mark migration routes.

On the southern side of the U.S./Mexico border, the state of Sonora experienced a significant number of weekly cases (Figure 13B).⁶⁰ As vectors accumulated along the border waiting for an opportunity to enter the U.S. (legally or illegally) from Latin America and beyond, chaotic backflow infected northern Mexico. The cities along the usual migration routes were most infected, as might be expected. One major line of infection stretched from the port of Cajeme Mex. (C. Obrigón) in the south to Guaymas Mex., passed through Hermosillo Mex., Santa Ana Mex., Nogales Mex./AZ, Tucson AZ, and terminated at Phoenix AZ in the U.S. Another stretched from Santa Ana Mex., to Cananea Mex., to Agua Prieta Mex. / Douglas AZ, and a third stretched from Santa Ana Mex., to Caborca Mex., to Sonoyta Mex., and up through Organ Pipe Cactus National Monument AZ (a favorite route for migrants entering the U.S. illegally). Finally, there was migration from Santa Ana Mex. through San Luis Rio Colorado, Mex. to the agricultural Fields of Yuma AZ. The Biden Administration claimed their border policy was "humane". *For whom, and what effect will millions of migrants have on the outcome of future elections in the U.S.?*⁶²

S. Korea: Due to its high population density, South Korea was once one of the most infected countries in the world, with total cases *per capita* exceeding many other industrialized nations (Germany, Italy, U.K., U.S., and Japan). France had only slightly more cases *per capita* according to Worldometer.⁶³ Yet, this industrialized Asian nation managed to bring a horrific COVID infection under control in just 13 months! How did they do it?

The infection history in South Korea can be broken up into three parts; an initial phase, a severe (omicron) phase, and a terminal phase. South Korea's patient zero appeared on January 19, 2020, about a month after the virus emerged in Wuhan, China. South Korea quickly implemented a containment strategy (Feb. 23, 2020) that did not depend on a full lockdown as in China, but instead relied on its experience from the 2015 MERS outbreak.⁶⁴ Key measures included: 1) an aggressive testing program employing "drive-thru" testing sites to screen a huge portion of the population (very innovative), 2) detailed contact tracing for confirmed cases, including the use of credit cards to track a vectors movements (very innovative) 3) government dissemination of information to the

public in real-time (transparent communications), 4) an aggressive vaccination program with 90% of adults fully vaccinated by November 2021. This program should be compared to containment efforts in the U.S.: 1) there were no “drive-thru” testing sites in the U.S. With few exceptions, temperatures were not even checked on inter-state highways as motorists crossed state borders, 2) contact tracing was largely confined to the local patient zero, 3) government dissemination of information was largely evasive, ambiguous, or incomplete, to avoid legal complications, 4) there was a lack of compliance by the general public with regard to vaccination, with just under 60% of the U.S. population fully vaccinated by Nov. 30, 2021 (not enough to achieve “herd immunity”).⁶⁵ The results speak for themselves – the U.S. had a massive outbreak of close to 10 million active case by November 2021, while simultaneously Korea had a relatively negligible case count. When will we ever learn? Since the pandemic seemed to be under control in S. Korea, the government relaxed its strict public health policy to a “Living with COVID-19” policy – *this was an incautious decision!*

Then something terrible happened that can be summed up in one word – *omicron!*⁶⁶ The strain was already in the U.S. in November, and although S. Korea began final testing of its own *SK biosciences* COVID-19 vaccine one month later in December, it was already too late!⁶⁷ Omicron had mutated too far, too fast, for the old vaccine formulations to have been very effective.⁴⁰ It was, in effect, a new disease! Figure 14 shows what happened during this phase of South Korea’s COVID-19 infection history. The number of daily new cases versus time rose sharply, and displayed three peaks whose origins seem easy to understand. Geographically, South Korea is surrounded on three sides by strictly monitored coastal waters, and a heavily guarded border to the north. Direct illegal entry into South Korea is rare. However, there is a significant legal migration into South Korea by seasonal workers (especially agricultural workers), international students and, of course, tourists. So, the warmer months from the beginning of April to the end of September are the

peak season for migration and, as people travel, they spread disease. Furthermore, South Korea has numerous air and sea links with China (see the $A_p(2,3)$ matrix element of Figure 6).⁶⁸ In fact, about one third of all migration comes from China. This was the source of S. Korea’s earliest infection.⁶⁹ In any case, it is not surprising to find a prominent summer peak in Figure 14. Climatically, Korea is very cold in the winter, with January temperatures often below freezing in Seoul.⁶⁸ Hence one would expect a strong thermal component in the daily new case profile as a function of time (season). A high population density combined with close industrial working conditions insure strong winter infection peaks, while bitter winters also favor migration during the summer months. However, as Figure 14 shows, each of the three infection peaks was sequentially reduced in size exponentially. Why? It is precisely because the South Korean government reinstated its strict public health policies, especially with regard to social distancing, limiting gatherings, and vaccine update.⁷⁰ This retightening occurred only one month after the S. Korean “Living with COVID-19” policy was put into place!⁷⁰

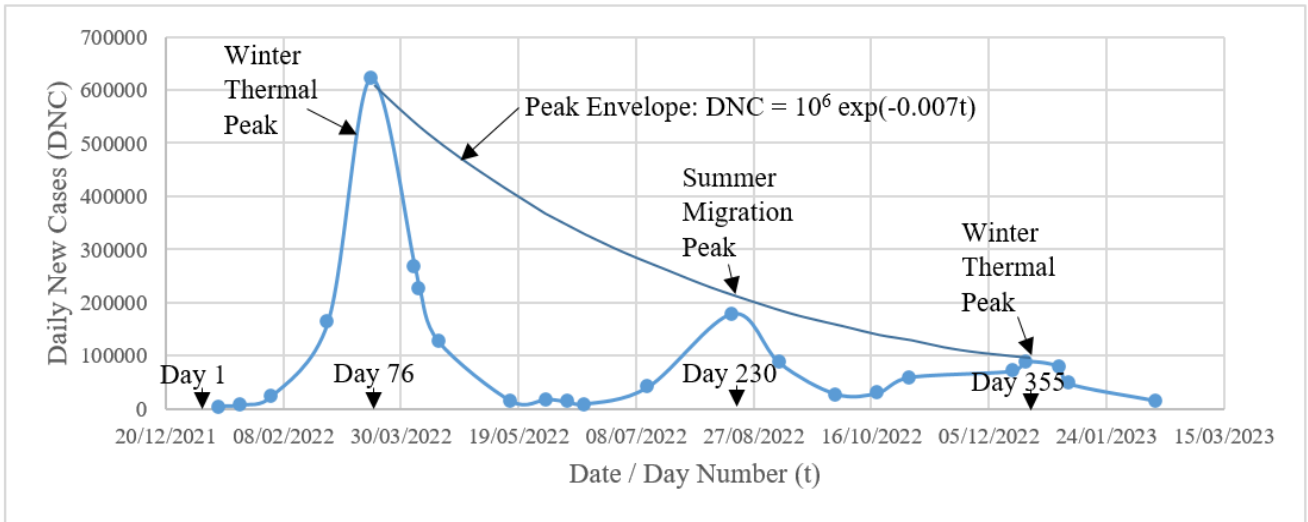


Figure 14 – Daily new cases versus time for South Korea.⁷¹ Peak heights (Daily New Cases – DNC) show an exponential decrease, where time *t* is the day number of the year, and New Year’s Day 2022 = day 1.

There is no secret as to how the Korean’s tamed COVID, and as of May 2024, people in Seoul were still vigilant even if the government didn’t require it (see Figure 15A)! Furthermore, as of that same date, all passengers flying into S. Korea from abroad were required to fill out a “Health Declaration Form”

(Figure 15B). Finally, it should be noted that the fatality rate from COVID in S. Korea was only 0.1%, compared to 1.2% in the U.S. The low fatality rate can be traced to the high rate of vaccination in S. Korea and the country’s outstanding and well-equipped hospital system.⁶⁶



A

B

Figure 15 A) This is something you will not see in the U.S. – a subway car full of riders all wearing masks. In Asia, there is no stigma attached to wearing masks in public places! Photo by the author on line 4 in Seoul, May 8, 2024. B) The “Health Declaration Form” required of all travelers flying into Korea (given to the author on May 5, 2024).

With the current relaxation of restrictions, COVID is on the rise again. S. Korea had 433 hospitalized COVID-19 patients from Aug. 31 to Sept. 6, 2025.⁷² Globally, XFG is the dominant strain, and accounted for 67% of sequenced cases for the week ending August 10, 2025.⁷³ The second most common strain is NB.1.8.1,⁷⁰ though its prevalence is decreasing; presumably it is being out-competed by XFG. Reliable and complete data on active COVID-19 cases is increasingly difficult to obtain as many governments and health organizations have scaled back surveillance efforts – *a big mistake!*⁷⁴

China: Although the COVID-19 pandemic started in China, few countries on Earth have done more to suppress its spread.⁷⁵ Briefly, here is how the “Zero-COVID Policy” worked. During the pandemic, if even one case of COVID appeared in a “neighborhood”, the entire neighborhood was quarantined. Some neighborhoods in Beijing have perhaps 5 or 10 thousand people because of the presence of high-rise apartments, but many neighborhoods in China are smaller. A resident of Beijing could check the quarantine status of their neighborhood on the internet – green indicated open (safe), while red indicated quarantine. If you ask the average person on the street in Beijing if this procedure worked to control the infection, that person will probably say, “NO!” Perhaps mathematics can shed some light on this response.

Let \mathcal{N} be the total number of people in a large population, and let m equal the number of people that each infected person can, in turn, infect in this same population. Furthermore, let this population be divided up into n neighborhoods that are completely isolated from one another in the sense that an infected individual in one neighborhood cannot infect someone in another, and let each neighborhood contain \mathcal{N} people, where $\mathcal{N} \ll \mathcal{N}$. If t is the total time elapse from the start of an infection (in either \mathcal{N} or \mathcal{N}) measured in days, and MICLP is the *mean incubation carrier latency period* (during which each vector attempts to infect m others), then as before $\tau \equiv t/\text{MICLP}$ is the dimensionless elapsed time measured in MICLP units of about 5 days each.

Starting with $\mathcal{N}_0 = 10$ infected people in a theoretically infinite population \mathcal{N} at $\tau = 0$, it would be found that the number of infections grows at a rate $10 m^\tau$. However, if those initial 10 people are uniformly distributed over $n = 10$ small neighborhoods of $\mathcal{N} = 100$ people (1/ neighborhood – a worst case), then growth of the infection will be slower because after each MICLP there will be less susceptible people left in a small neighborhood, since each infected person will either die (not likely) or recover and become immune (likely). Now the infection within *each neighborhood* will grow as the sequence $1, (99/100)m, \{[100 - (99m/100 + 1)]/100\}(99m/100)m, \dots$ etc. as a function of τ ,⁴⁰ and the infection for *all ten neighborhoods* will grow as 10 times this sequence. As a realistic example let $m = 3$, then Figure 16 emerges. Notice that the reduction in the total number of infections is 16.85% after only 3 MICLP time units (~ 15 days), and this reduction will grow as τ continues to increase. The question the reader must ask is, “Will the average citizen notice such a drop?” The answer is, “probably not.” However, to a COVID nurse running out of hospital beds, an improvement of almost 17% could be life-saving! Although *initially* successful from a purely mathematical and medical point of view, the Zero-COVID Policy faced significant challenges as more transmissible variants like omicron emerged. This strain was so contagious that it became impossible to define an isolated self-contained neighborhood. There was no such thing as far as omicron was concerned! Challenges to the Zero-COVID Policy also came from the public, because there is more to fighting a pandemic than infection statistics alone. Isolation leads to economic loss, collateral mental and physical health issues, and social unrest. Anti-Zero-COVID Policy demonstrations had been reported in several cities in China.⁷⁶ It is difficult to say just how effective these demonstrations were in convincing the government in Beijing to change its strict COVID policy. A demonstration in China is not the uncontrolled mob that it is in the U.S. Demonstrations are by permit only, and are limited in size. Nevertheless, the mere existence of such a demonstration might send a message to the PRC government that it needs to address an urgent issue.

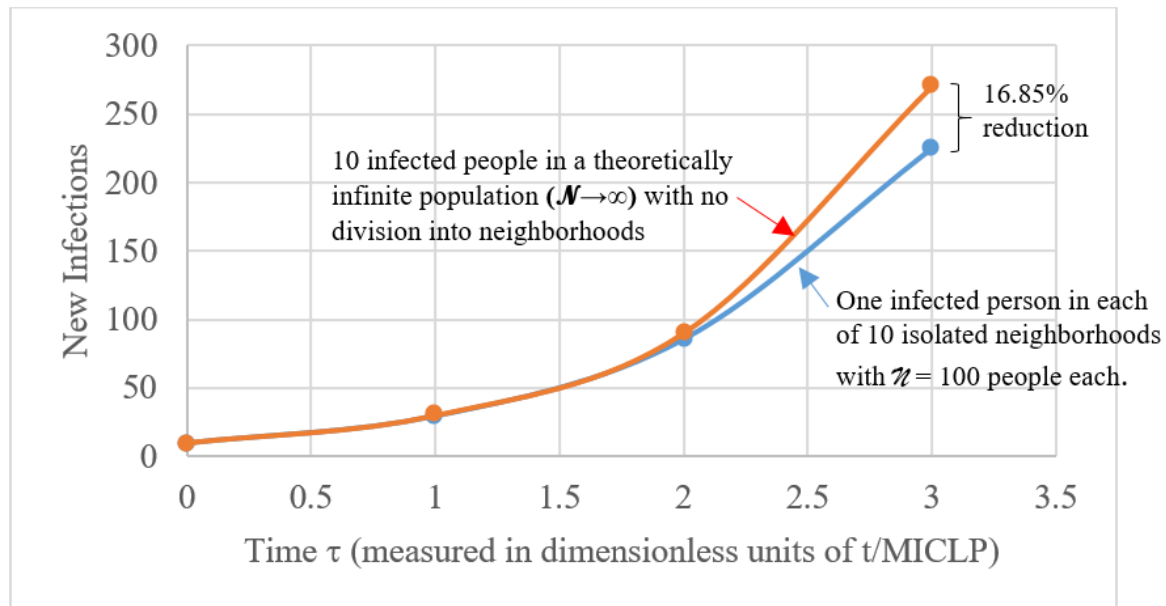


Figure 16 – The reduction in the number of infections due to division of a large population into “neighborhoods” as a function of $\tau = t/\text{MICLP}$. Each MICLP time unit represents about 5 days, the incubation carrier period. After that an infected individual will show symptoms and be considered isolated until recovery and immunity. The next infection cycle begins with the people infected in the previous cycle, etc.

India: “We let our guard down when the variants were spreading. It was the worst time to do so.” – those were the words of T. Jacob John, a virologist working in Vellore, India.⁷⁷ By Apr 2021 the Delta variant was spreading, and India was caught with its masks down. As previously discussed, the same thing happened in S. Korea with the omicron strain just 7 months later. A similar mistake was made in the U.S.⁷⁸ The take-away from these examples is obvious: *even if public health authorities think an epidemic or a pandemic has run its course, there needs to be a delay in the repeal of strict public health measures.* A year of continued vigilance would not have been unreasonable for COVID because of the rate at which this virus was mutating. Had this been done, much of the pain of the Delta and omicron strains could have been avoided.

Turkey: This was one of the few countries in the world that was largely spared the ravages of COVID – up until March 4, 2020.²⁴ How did they do it? The answer is simply that they immediately closed their eastern border to travelers. Before the first confirmed case in Turkey, Iran already had 43 cases with eight deaths.

That was enough to prompt Turkey to close all four of its land border gates, and suspend all train and flight service with Iran as a preventative measure.⁷⁹ In fact, even before closure, Turkey had already intensified precautions at the border. Authorities in Van, a popular destination for Iranian tourists in eastern Turkey, installed thermal cameras at the Kapiköy border crossing, while border officers in contact with visitors were ordered to wear protective gear.⁷⁹ Amazingly, Turkey also successfully evacuated 32 Turks from Wuhan on Jan 26, 2020. Although these proactive measures may not have stopped the COVID infection completely, they were successful at slowing the spread of the virus sufficiently to keep it under control until vaccines became available. *Clearly, prompt early action together with a sensible border policy were very effective!*

The Navajo Nation / U.S.: Although not usually thought of as a separate nation because it lies within the U.S., the *Diné* (Navajo people) of the isolated “four corners” area of the American Southwest are the largest Native American population in the lower 48 states. They had been hit hard by COVID

because, as in the case of measles, they were exquisitely susceptible to this novel Old World disease.⁸⁰ COVID first appeared on the reservation on Mar. 17, 2020, and by August 6, 2021, a total of 31,572 people had been infected - about 7.9 % of the *Diné* in just 16 months – with 1,893 deaths.⁸¹ In

fact, in 2020, the Navajo Nation had a higher per capita rate of infection than any state of the U.S. So, there was little or no opposition to vaccination or other public health measures in Navajo Lands (Figure 17).



Figure 17 – On the Navajo reservation, the campaign to get everyone vaccinated was intensive. From roadside billboards (left) to free restaurant vaccination pins (right), the *Diné* were serious about beating this new biological threat to their population. Where was this level of commitment in the rest of the U.S.? Photo by author; July 5, 2025.

The first doses of vaccine to be prepared were emergency air shipped to reservations in the U.S. by the Trump Administration.⁸² By May 26, 2021, 70% of the *Diné* had been *fully vaccinated*,⁸³ compared to just under 40% for the total U.S. population,⁸⁴ and by August 3, 2021, there were only 15 cases of delta (the dominant strain at that time) among the *Diné*,⁸⁵ and 28 new cases counting all strains;⁸⁶ out of about 400,000 enrolled tribal members in 2021. Mask wearing was common to almost universal, road closures into and across Navajo lands were common, and admission to stores was on a “need-to-buy” basis – as usual, the author was on the spot observing directly. Even a single new case of COVID in a High School made the front page of the Navajo Times on August 5.⁸⁷ When the small daily infection rate of 0.0070% among the *Diné* (28/400,000) is compared to the national number of 103,455 new COVID cases on August 3, 2021,⁸⁸ or 0.0307% of the population (assuming 337 million Americans), one realizes that much of the COVID blood-bath seen in the U.S. could have been avoided if the general population had been as enlightened and

compliant as the *Diné*! However, the combination of media misinformation, lack of cooperation due to political rivalry, and ineffective distracted leadership that chose not to make the pandemic a national priority, all took their toll – perhaps resulting in 4.4 times more infections than necessary (0.0307/0.0070).

The Lockdown–Economics, Vaccination, and Rumors: Although the Earth has now been rounded again in this section, there is one last lesson learned by all nations of the globe – the economic lesson. Much has been made about economic loss in the press, and certainly some of the weaker business were bankrupted by the Lockdown. However, the economic fallout might not have been as great as touted by the press, who seem to enjoy blaming the lockdown for almost anything economic years later.⁸⁹ Looking at the facts tells a different story. Figure 18 below shows the Dow Jones Industrial Average (DJIA) during the COVID pandemic. Clearly, the effect in the U.S. was serious, but it was also short lived. In China, where the Lockdown was considerably more inconvenient than in the U.S., there was a record

trade surplus in 2021, as that country accounted for one third of all the imports and exports in the Asia-Pacific region.⁷⁵ Furthermore, unemployment in China was fairly stable from Jan. 2019 to May 2023, and was almost equal to that before the pandemic.⁷⁵ In S. Korea, the gross domestic product growth rate was -1.0% in 2023, but within a year exports

rebounded and corporate investment expanded.⁹⁰ Additionally, the Gross Domestic Product of the US, EU, and China was, on the average, growing from the first quarter of 2019 to the first quarter of 2023.⁷⁵ Globally then, the impact of the lockdown does not seem to have been catastrophic.

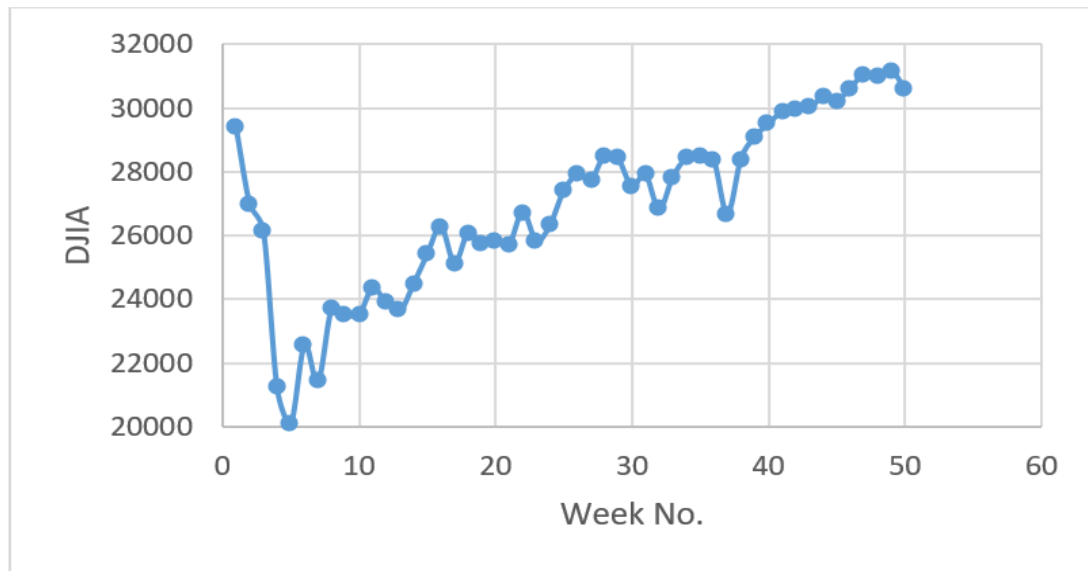


Figure 18 – The Dow Jones Industrial Average (DJIA) during the early stages of the pandemic in the U.S. Data were taken on Thursdays from Feb. 20, 2020 to Jan. 28, 2021 at one week intervals. The initial decline was deep (about 30%) and rapid, but the market had fully recovered within about 40 weeks at an almost linear rate.

These figures raise two compelling, and related, questions. First, was the Lockdown worth it? Second, perhaps more interestingly, why did so many people in the U.S. forego vaccination, resist public health measures, and believe ridiculous rumors with regard to the prevention and treatment of COVID during the lockdown? *Worth* is always difficult to define, because it is a subjective term. However, it must always be remembered that in the early days of the pandemic, no one was really sure what they were dealing with. *Fear* seems to have been the driving force behind the Lockdown. Once a vaccine became available, that *fear* was mitigated. The author doesn't have a completely satisfactory answer to the second question. Although a few observations seem relevant. If vaccination is what mitigated fear, then why was there such resistance to that procedure? Perhaps COVID wasn't *deadly enough* to frighten everyone into compliance, as it did in the Navajo Nation? Perhaps there was enough *hope* of not being

infected, or of surviving such an infection if one were unlucky, to make foregoing vaccination an option? Resistance to vaccination is not new. It began in the late 18th century and continued through the polio epidemic of the 1950's in the U.S.. Before Jenner's pioneering use of relatively harmless cow pox to vaccinate against human small pox (1796), vaccination had been practiced by exposing a healthy person to the infectious material of a virulent human disease via a non-standard route of infection. The procedure usually worked, but the failure rate was high, and so was the fear of vaccination. Perhaps this is the original source of the vaccination fears that are still so prevalent today. It is not unusual for myths, fears, and rumors to persist for hundreds, or even thousands, of years. Here in the U.S., resistance to vaccination seems to have followed political lines. "Conservatives" seem to have shown more resistance than "liberals", whatever those labels might mean. What is so bizarre is that the COVID vaccine program

in the U.S. was initiated by President Trump – a very conservative president. How it came to pass that political loyalties became reversed on this one issue is a political Ju-Jitsu trick that the author is at a loss to understand or explain. What about public health measures like wearing masks? This also seems to have followed political lines. People in the U.S. who had the money to invest, people who would normally be considered “conservative”, obviously believed that COVID was a threat to the nation’s economy if it produced a 30% market decline – an event that occurred only four times in the last 100 years! Yet, it is precisely the politically conservative segment of society that was most resistant to public health measures. Perhaps conservatives felt that such measures would hurt profits? However, such an argument makes little sense on a personal level. In any case, what Rebecca Lemove, historian of science, calls “hyper-persuasion” set in.⁹¹ People became objects of ridicule if they wore a face mask, and the natural human desire for acceptance superseded their common sense. Soon, almost no one in the U.S. wore a face mask – regardless of whether they were liberals or conservatives. Hyper-persuasion also played a key role in the spread of rumors about prevention and treatment. The internet, television, radio, and the press all played their part in the spread and acceptance of rumors – what Lemove calls technological behavior change. Orange juice is not going to keep you from getting COVID, nor is vaccination going to give you “mad cow disease”. Yet, all of these falsehoods that play on the emotions of hope and fear, could be found in the media, and reinforcement by repetition from friends completed the cycle of hyper-persuasion.⁹¹

Conclusion

In 1905, the Spanish-American philosopher George Santayana penned his much quoted and now famous proverb, “those who do not remember the past are condemned to relive it.” Indeed, the purpose of any history is to identify the successes and failures of our actions; thereby highlighting those things that we could have done to mitigate a draconian situation, outcome, or both. So, let’s build two lists.

One for what we did right. The other for the things that we did that were wrong. These lists will give us a pretty good idea of how we should prepare for the next pandemic and, in a world of 8 billion people that are so connected together and concentrated along the coasts (40% live within 100 miles of a coast), there *will* be other pandemics.

1) Right: The successful recall of Turkish citizens from Wuhan shows that a direct flight, with the quarantine of travelers for the incubation carrier latency period (~ 5 days for COVID) prior to departure, followed by an equivalent isolation after arrival, is a doubly redundant, almost fail-safe way to move people across international borders. Establishing the incubation carrier latency period is the primary and immediate task of public health authorities upon the outbreak of a new disease.

2) Wrong: Cancelling direct non-stop flights from infected nations. Unless all incoming flights are stopped, this just forces travelers into indirect paths where the risk of spreading infection grows exponentially with the number of stops (layovers) involved, and where monitoring along the way may be lax, or non-existent.

3) Right: The immediate and effective closure of land borders with Iran was effective in slowing the spread of COVID into Turkey. When it comes to border closure, *time is of the essence*.

4) Wrong: Maintaining an open, or lax, border policy. This resulted in massive COVID outbreaks along the U.S./Mexico border.

5) Right: In the case of respiratory infections, maintain strict public health measures for a full annual cycle *after* the peak of the epidemic or pandemic is believed to have past.

6) Wrong: Prematurely drop strict public health rules and data collection for political, psychological, or economic reasons. The U.S., India, and S. Korea, all fell into this trap!

7) Right: Be vigilant about contact tracing using the innovative methods pioneered in South Korea. Even a single infection in a remote country can affect the long-term course of a pandemic via the “butterfly

effect". In this regard, establishment of regional stockpiles of emergency supplies in the non-industrialized world is vital for global protection.

8) *Wrong:* Ignore the emergency medical needs of underdeveloped nations because they are "remote". This is a policy that, given enough time, will recoil on everyone - like germ warfare. If m is large enough, no nation is remote! At present, the WHO (World Health Organization) provides recommendations for stockpiling, but individual countries are responsible for establishing their own national reserves, which are often (but not always) regionally coordinated.^{92,93}

9) *Right:* Make compliance with public health measures a "campaign", as it was within the Navajo Nation and South Korea. There is no doubt that such measures were successful.

10) *Wrong:* Spend billions of dollars on political campaigns, but prematurely reduce spending on emergency public health measures.⁹⁴

11) *Right:* Lockdown, and isolation measures to be taken, should depend on both the lethality and infectiousness (m) of any disease.

12) *Wrong:* Not Locking-Down when a disease is known to have both high lethality and infectiousness, or when lethality and infectiousness parameters are unknown, could be disastrous. On the other hand, Locking-Down when neither lethality or infectiousness are high might do more harm to the public's physical, mental, and economic health, than it's worth. This is a very difficult decision.

In hind-sight, it is clear that many aspects of the COVID-19 pandemic can be understood in mathematical detail, even on a global scale. However, mathematics also defines the limits to what can be known as well. Perhaps most importantly though, mathematics gives a clue as to what can be expected in the future, regardless of whether the next pandemic involves a coronavirus strain or some other microbe, and what might be done to mitigate its effects.

References:

- 1) United Nations World Health Organization (UN WHO). *WHO-convened Global Study of Origins of SARS-CoV-2: China Part: Joint WHO – China Study*. 14 January – 10 February 2021: Joint Report. WHO 2021. Accessed December 1, 2025 <https://www.who.int/publications/i/item/who-convened-global-study-of-origins-of-sars-cov-2-china-part>
- 2) Xixing Li, Weina Cui, Fuzhen Zhang. Who Was the First Doctor to Report the COVID-19 Outbreak in Wuhan, China. *J. Nuc. Med (JNM)*. June 2020; 61(6): 782-783. DOI:10.2967/jnumed.120.247262; PMID: PMC7262218; PMID: 32303602. Published online Apr. 17, 2020. Accessed July 20, 2025 <https://www.pmc.ncbi.nlm.nih.gov>
- 3) M. Worobey. Dissecting the early COVID-19 cases in Wuhan. *Science*, Nov. 18, 2021; 374(6572): 1202-1204. DOI: 10.1126/science.abm4454. Accessed July 20, 2025 <https://www.science.org>
- 4) Worldometer. *COVID – Coronavirus statistics*. Accessed Jan. 24, 2025 <https://www.worldometers.info>
- 5) Japan Air Lines. *JAL, Routes/Flight Information, East Asia*. Accessed Jan. 25, 2025 <https://www.jal.co.jp>
- 6) Air China. *Air China Flights and Destinations*. Accessed Jan 25, 2025 <https://www.flightconnections.com>
- 7) Korean Air. *Korean Air (KE/KAL) routes and destinations*. Accessed Jan. 25, 2025 <https://www.flihtadar24.com>
- 8) Korean Air. Korean Air International Route Map, Korean Air East Asia Route Map. *MORNINGCALM*. May/June 2024: 46-49.
- 9) Delta Air Lines. Route Map | Delta Air Lines, Images (including maps for March 2020). Accessed Jan. 25, 2025 <https://www.delta.com>
- 10) British Airways. British Airways Flights and Destinations – Flight Connections, Images. Mar. 7, 2025. Accessed July 20, 2025 <https://www.flightconnections.com>
- 11) Air France. Air France Flights and destinations, Images. July 3, 2025. Accessed July 20, 2025 <https://www.flightconnections.com>
- 12) Lufthansa. Lufthansa Flights and Destinations, Images. July 3, 2025. Accessed July 20, 2025 <https://www.flightconnections.com>
- 13) Stone W. 1st U.S. Case Of Coronavirus Confirmed In Washington State. Jan. 22, 2020, *NPR*, Accessed Feb. 25, 2025 <https://www.npr.org>,
- 14) Robison P, Bass D, Langreth R. How Coronavirus Spread From Patient Zero in Seattle. *Bloomberg*, Mar. 9, 2020. Accessed Feb. 25, 2025. <https://www.bloomberg.com>. Also, *Businessweek*, March 16, 2020.
- 15) Ryan H, St. John P, Liang X. The surprising story of the salesman who became L.A.'s first known COVID-19 patient. *Los Angeles Times*, Aug. 21, 2020. Accessed July 31, 2025 <https://www.latimes.com>
- 16) Anon. U.S. Announces China Coronavirus Travel Ban. *Dorsey + Whitney LLP*, Feb. 1, 2020 (updated Mar. 3, 2020). Accessed July 20, 2025 <https://www.dorsey.com>
- 17) Zito R.R. COVID-19. *J. of Sys. Safety*. Fall/Winter 2020; 56(2): 10-25.
- 18) CDC, About Traveler-based Genomic Surveillance, May 14, 2025. Accessed July 20, 2025 <https://www.CDC.gov>
- 19) Kesslen B. New York area's 'patient zero' says coronavirus 'wasn't on my mind' when he got sick. *NBC News*. May 11, 2020. Accessed July 21, 2025 <https://www.nbcnews.com>
- 20) Brody L. Covid-19's 'Patient Zero' in New York: What Life is Like for the New Rochelle Lawyer. *Wall Street Journal*. Updated March 5, 2021. Accessed July 21, 2025 <https://www.wsj.com>
- 21) World Health Organization (WHO). COVID-19 – United Kingdom of Great Brittan and Northern Ireland. *Disease Outbreak News*. Dec 21, 2020. Accessed July 21, 2025 <https://www.who.int>
- 22) Zárate S. et al. The Alpha Variant (B.1.1.7) of SARS-CoV-2 Failed to Become Dominant in Mexico. *National Institute of Health (NIH), National Library of Medicine (NLM), PubMed Central (PMC)*. Accessed July 21, 2025 <https://www.pmc.ncbi.nlm.nih.gov>. Also see, *Microbiol. Spectr.* Apr. 7, 2022; 10(2): e02240-21. DOI: 10.1128/spectrum.02240-21
- 23) Journalist's Resources. The Problem with 'Patient Zero' in Coronavirus News. *Boston University School*

- of Public Health. Apr. 6, 2020. Accessed July 22, 2025 <https://www.bu.edu>
- 24) Letzing J. Finding 'patient zero: the challenges of tracing the origins of coronavirus. *World Economic Forum, Health and Healthcare Systems*. Mar 4, 2020. Accessed July 22, 2025 <https://www.weforum.org>. Note the video image "Spread of COVID-19 globally".
- 25) Bastola A. et al. The first 2019 novel coronavirus case in Nepal. *The Lancet*. March 2020; 20(3): 279-280. Accessed July 21, 2025 <https://www.thelancet.com>
- 26) Anon. India's Patient Zero Tests Positive For Coronavirus Again: Report. *Kerala News*. July 13, 2021. Accessed July, 21, 2025 <https://www.ndtv.com>
- 27) Zahid A. Meet Patient Zero: Syed Yahya Jafri. *Aurora Magazine – People*. Mar-Apr 2021. Accessed July 21, 2025 <https://aurora.dawn.com>
- 28) Anon. Iran: 43 infected with coronavirus; patient zero identified. *Middle East Monitor (MEM)*. Feb. 23, 2020. Accessed July 22, 2025 <https://middleeastmonitor.com>
- 29) Alfoneh A. Iran's Patient Zero: The Islamic Republic. *Arab Gulf States Institute (AGSI), Politics and Governance*. March 3, 2020. Accessed July 22, 2025 <https://agsiw.org>
- 30) Reuters. Coronavirus: Turkey reports first case of COVID-19. *Middle East Eye*. Mar. 10, 2020. Accessed July 22, 2025 <https://www.middleeasteye.net>
- 31) Wikipedia. COVID-19 pandemic in Spain. Accessed July 22, 2025 <https://en.wikipedia.org>
- 32) Laguipo A. First French COVID-19 case was in December 19. *News-Medical*. May 5, 2020. Accessed July 22, 2025 <https://www.news-medical.net>
- 33) Anon. Who is 'patient zero' of COVID-19 pandemic? Here's what we know. *CGTN America*. March 30, 2020. Accessed July 21, 2025 <https://www.america.cgtn.com>
- 34) Devlin H. No 'patient zero' as Covid-19 came to UK at least 1,300 times. *The Guardian*. June 11, 2020. Accessed July 21, 2025 <https://www.theguardian.com>
- 35) Zito RR. The Omicron Strain: An Overview of Its Growth and Decline in the U.S. *Medical Research Archives*. Jan. 30, 2025; 13(1): 1-26. <https://doi.org/10.18103/mra.v13i1.6069>
- 36) Marshall CW. *Applied Graph Theory*. Wiley-Interscience, New York, N.Y., 1971:8, 9, 178, 258.
- 37) Selby SM. *Standard Mathematical Tables*, 16th ed. The Chemical Rubber Co., Cleveland, OH, 1968: 108.
- 38) Ross IC, Harary F. On the determination of redundancies in sociometric chains. *Psychometrika*, 1952; 17:195-208.
- 39) Zito RR. *Mathematical Foundations of System Safety Engineering*, Springer Nature, Switzerland, 2020: 105-112, 146-147.
- 40) Zito RR. The Omicron Strain: An Overview of its Growth and Decline in the U.S. *The European Society of Medicine, Medical Research Archives*. Jan. 30, 2025; 13(1): 1-26. Available on-line at <https://doi.org/10.18103/mra.v13i1.6069>
- 41) Khmara D. Migrant encounters on rise at Arizona-Mexico border. *Arizona Daily Star*. June 18, 2022: A1, A2.
- 42) Khmara D. End of Title 42 could overwhelm Pima County. *Arizona Daily Star*. Apr. 5, 2023: A1, A4.
- 43) Ray M. Madrid train bombings of 2004. *Britannica*. Updated Jan. 25, 2025. Accessed Jan. 25, 2025 <https://www.britannica.com>
- 44) Carassava A. Greece Alarmed by Rising Tides of Migrants. *VOA News*. March 17, 2024 <https://www.voanews.com>
- 45) Dor G, et al. Tracing the spatial origins and spread of SARS-CoV-2 Omicron lineages in South Africa. *Nature Communications*. May 28, 2025; 16: 4937. Accessed Nov. 10, 2025 <https://www.nature.com>
- 46) Peitgen HO, Richter PH. *The Beauty of Fractals*. Berlin: Springer-Verlag; 1986: 23-26.
- 47) Lynch WA, Truxal JG, *Introductory System Analysis*. New York, NY: McGraw-Hill; 1961: 288.
- 48) Lorenz EN. Deterministic Nonperiodic Flow. *J. Atmospheric Sci*. 1963; 20: 130-141.
- 49) Ning CZ, Haken H. Detuned lasers and the complex Lorenz equations: subcritical and supercritical

- Hopf bifurcations. *Phys. Rev. A*, 1990; 41(7): 3826-3837. Bibcode: 1990PhRv..41.3826N, doi: 10.1103/PhysRevA.41.3826, PMID 9903557
- 50) Hemati N. Strange attractors in brushless DC motors. *IEEE Transactions on Circuits and Systems 1: Fundamental Theory and Applications*. 1994; 41(1): 40-45. Bibcode: 1994ITCSR..41...40H, doi: 10.1109/81.260218, ISSN 1057-7122
- 51) Poland D. Cooperative catalysis and chemical chaos: a chemical model for the Lorenz equations. *Physica D*, 1993; 65(1): 86-99. Bibcode: 1993PhysD...65...86P, doi: 10.1016/0167-2789(93)90006-M.
- 52) Cuomo KM, Oppenheim AV. Circuit implementation of synchronized chaos with applications to communications. *Physical Review Letters*. 1993; 71(1): 65-68. Bibcode: 1993PhRvL..71...656, doi: 10.1103/PhysRevLett.71.65, ISSN 0031-9007, PMID 10054374.
- 53) Anon. Lorenz System. *Wikipedia*. Accessed Nov. 11, 2025 <https://en.wikipedia.org>
- 54) Taylor J (writer, producer, and director). *The Strange New Science of Chaos*. Nova, WGBH Educational Foundation, WGBH Boston, 1999.
- 55) Miller Z, Perrone M. U.S. likely to authorize COVID booster shots. *Arizona Daily Star (Associated Press release)*. August 18, 2021: A1, A2.
- 56) USCBP. Southwest Land Border Encounters by Month. *U.S. Customs and Border Protection*. 2023. Accessed Mar. 16, 2023 <https://www.cbp.gov>
- 57) Hatfield J. Q&A: How Pew Research Center estimates the number of unauthorized immigrants living in the U.S. *Pew Research Center*. Aug. 22, 2025. Accessed Sept. 16, 2025 <https://www.pewresearch.org>
- 58) USAFacts. How many people immigrate to the US via authorized channels each year? *USAFacts*. June 6, 2024. Accessed Sept. 16, 2025 <https://usafacts.org.org>
- 59) Smart C. Covid Hospitalizations Hit Crisis Levels in Southern I.C.U.s. *New York Times*. Sept. 18, 2021: A1.
- 60) Gobierno del Estado de Sonora (Government of the State of Sonora). Informe Epidemiológico COVID-19, Sonora 2022: Municipios con mayor riesgo de transmisión de COVID-19 (Actualización semenal). (COVID-19 Epidemiological Information, Sonora 2022: Municipalities [i.e. counties] with a major risk of transmission of COVID-19 – Updated weekly.) *Unidad Detectora De Urgencias Epidemiológicas (UDUE). (Epidemiological Emergencies Detection Unit)*. May 16, 2022. Accessed Nov. 27, 2025 <https://salud.sonora.gob.mx>
- 61) Anon. Template: COVID-19 testing by country. *Wikipedia*. Accessed Dec. 2, 2025 <https://en.wikipedia.org>
- 62) Kim SM, Groves S. Half a million immigrants could eventually get citizenship under a sweeping new plan from Biden, AP News. June 18, 2024. Accessed Nov. 27, 2025 <https://apnews.com>
- 63) Worldometer. COVID – Coronavirus statistics. Accessed Mar. 30, 2023 <https://www.worldometers.info>
- 64) Cha V, Kim D. A Timeline of South Korea's Response to COVID-19 – CSIS. *CSIS (Center for Strategic and International Studies)*. Mar. 27, 2020, <https://www.csis.org>
- 65) Pariseault AB. Current Status of COVID-19 Vaccine Rollout Nationwide: November 2021 Update for the Attorney General Community. *National Association of Attorneys General*. Dec. 2, 2021. Accessed Sept. 16, 2025 <https://www.naag.org>
- 66) Wikipedia. COVID-19 pandemic in South Korea. Last edited Sept. 8, 2025. Accessed Sept. 9, 2025 <https://en.m.wikipedia.org>
- 67) Anon. Final testing of Korean COVID-19 vaccine begins. *Korea Herald*. December 21, 2021. Accessed May 3, 2024 <https://news.koreaherald.com>
- 68) Harper D, Morgan M, O'Malley T, Tang P, Whyte R. *Korea*. Lonely Planet. 2021: 40, 395.
- 69) Kang YJ. South Korea's COVID-19 Infection Status: From the Perspective of Re-positive Test Results After Viral Clearance Evidence by Negative Test Results. *Disaster Med Public Health Prep*. Dec. 2020; 14(6): 762-764. PMID: 32438941, PMCID: PMC7298089, DOI: 10.1017/dmp.2020.168. Accessed Sept. 9, 2025 <https://pubmed.ncbi.nlm.nih.gov>

- 70) Shin H. South Korea to restore tougher curbs against spike in COVID-19 infections. *Reuters*. Dec. 16, 2021 <https://www.reuters.com>
- 71) Worldometer. South Korea – Coronavirus Cases. Accessed Apr. 24, 2024 <https://www.worldometers.info>
- 72) Seong-ho. 10-week Covid-19 surge ahead of Chuseok. *THE CHOSUN Daily*. Sept. 16, 2025. Accessed Nov. 30, 2025 <https://www.chosun.com>
- 73) WHO Data. WHO COVID-19 dashboard. *WHO Health Emergencies Programme*. Accessed Sept. 6, 2025 <https://data.who.int>
- 74) WHO. COVID-19 - Global Situation. Disease Outbreak News. *World Health Organization*. May 28, 2025. Accessed Sept. 6, 2025 <https://www.who.int>
- 75) Ba Z. et al., Reflections on the dynamic zero-COVID policy in China. *Preventative Medicine Reports*. Dec. 2023; vol. 36 Accessed Aug. 23, 2025 <http://sciencedirect.com>, <https://doi.org/10.1016/j.pmedr.2023.102466>
- 76) Burki T. Moving away from zero COVID in China. *Lancet Respir. Med.* Feb. 2023; 11(2): 132. Available on-line at <https://www.sciencedirect.com> and [https://doi.org/10.1016/S2213-2600\(22\)00508-2](https://doi.org/10.1016/S2213-2600(22)00508-2)
- 77) Li S, Agarwal V. " 'Double Mutant' Variant Hits India Hard", *The Wall Street Journal*. Vol. CCLXXVII, No. 95, Apr. 24-25, 2021: A7.
- 78) Hall D. "U.S. Cases Top 70,000 As Variant Spreads", *The Wall Street Journal*. Vol. CCLXXVII, No. 86, Apr. 14, 2021: A7.
- 79) Anon. Turkey closes border with Iran amid coronavirus concerns. *Daily Sabah* ('Sābāh' means 'Morning' in both Turkish and Arabic). Feb. 23, 2020. Accessed Sept. 10, 2025 <https://www.dailysabah.com>
- 80) Kakol M, Upson D, Sood A. Susceptibility of Southwestern American Indian Tribes to Coronavirus Disease 2019 (COVID-19). *J. Rural Health*. June 1, 2020; 37(1): 197-199. DOI: 10.1111/jrh.12451, PMID: PMC7264672, PMID: 32304251. NIH National Library of Medicine accessed August 27, 2025 <https://pmc.ncbi.nlm.nih.gov>
- 81) Wikipedia. COVID-19 pandemic in the Navajo Nation. August 6, 2021, Updated Dec. 2022. Accessed August 26, 2025 <https://en.m.wikipedia.org>
- 82) Oxner R. First Coronavirus Vaccine Doses Administered In Hard Hit Indigenous Communities. NPR. Dec. 17, 2020. Accessed Jan. 13, 2024 <https://www.npr.org>
- 83) Hatzipanagos R. How Native Americans launched successful coronavirus vaccination drives: 'A story of resilience'. *The Washington Post*. May 26, 2021. Accessed Jan. 11, 2026 <https://www.washingtonpost.com>
- 84) Pariseault AB. Current Status of COVID-19 Vaccine Rollout Nationwide: May 2021 Update for the Attorney General Community. *National Association of Attorneys General*. May 25, 2021. Accessed Sept. 16, 2025 <https://www.naag.org>
- 85) Becenti. Concern grows, Delta variant infections rise. *Navajo Times (Diné Bi Naaltsoos – "The People's Paper"* when literally translated from the Navajo language). Aug. 5, 2021: A1, A4.
- 86) Fonseca F, et al. Navajo Nation: No COVID-related deaths for 3rd day in a row. *Associated Press*. August 3, 2021. Accessed August 26, 2025 <https://KUTV.com>
- 87) Quintero D. Student tests positive. *Navajo Times (Diné Bi Naaltsoos)*. Aug. 5, 2021: A1. A3.
- 88) CDC, NIH. New Cases Reported to CDC on 8/3/21. *COVID-19 Press Briefing*. August 5, 2021. Accessed August 26, 2025 <https://bidenwhitehouse.archives.gov>
- 89) Derby MS. Fed data suggests central bank has stopped losing money. *Reuters*. Dec. 3, 2025. Accessed Dec. 3, 2025 <https://www.reuters.com>
- 90) Park HK. IMF: 'Korea's very successful COVID-19...minimizing reverse (economic) growth among the G20 (nations)'. (Note: Although this title is a rough colloquial translation from Korean by the author, the body of the article is in both Korean and English. The literal translation of Korean (a phonetic language) to English is awkward because there are no articles, and the word order is different, with the verb

appearing at the end of a sentence as in German.)

Korea Duty Free News. Updated May 7, 2024.

Accessed on-line in Korea on May 7, 2025

<https://www.kdfnews.com>

Korean Title: IMF “한국, ^{“k” sound}코로나19 대응 성공적... G20 중 역성장 최소화”
Korea's COVID-19 very successful among reverse growth minimizing

Author (Korean): 박 홍 규 = Hong Kyu Park

P ä k (usually rendered as “Park” in English, the 3rd most popular surname in Korea and shared by 8.4% of the population)

91) Lemov R. *The Instability of Truth - Brainwashing, Mind Control, and Hyper-persuasion*. New York, NY: W.W. Norton and Co.; 2025.

92) WHO. *Stockpiling of Medical Countermeasures for Pandemic Influenza*. Undated Draft. Accessed Dec. 16, 2025 <https://cdn.who.int>

93) WHO, Strategic plan for coronavirus disease threat management: advancing integration, sustainability, and equity, 2025-2030. December 2, 2025. Accessed December 18, 2025

<https://www.who.int>

94) Cochrane E. Democrats Strip Covid Aid From Spending Bill. *New York Times*. March 10, 2022: A1, A19.